Enhanced Control by Visualisation of Process Characteristics: Video Monitoring of Coal Powder Injection in a Blast Furnace

Jihad Daoud, Igor Nipl

Civilingenjörsprogrammet

Institutionen för Systemteknik
Avdelningen för Reglerteknik

2000:076 • ISSN: 1402-1617 • ISRN: LTU-EX--00/076--SE

Enhanced Control by Visualisation of Process Characteristics: Video Monitoring of Coal Powder Injection in a Blast Furnace

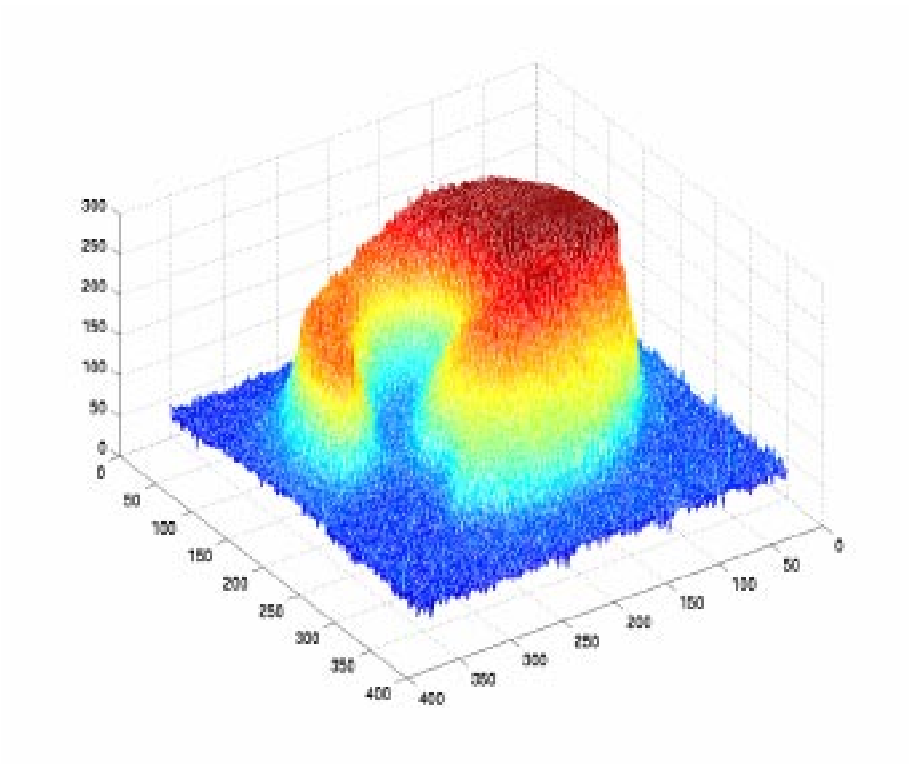

Jihad Daoud

Igor Nipl

2000-02-29

Authors address:

Luleå University of Technology
Department of Computer Science and Electrical Engineering
Control Engineering Group
S-971 87 LULEÅ, Sweden

`jihdao-6@student.luth.se`
`igonip-6@student.luth.se`

People come and go in our lives, so does every coal particle in a blast furnace. Some day you will become coal, and if you are lucky, you might be used in a blast furnace.
Nothing is static, not us, not you, not any of the images we analysed. Fighting against changes, being static, is like .... No opinion on that one!
A language can be used to control people, a computer can be used to control much more. It is only stupid people/things that are easy to control, but again everything is relative.
Do not ask us about the truth, we are still searching. When we find it, you will know it or you are already dead. If you are not dead, you are too lazy or you know something we do not know.

To the poor people.
"Jihad"
To Linda and my parents.
"Igor"

Abstract

This master thesis, based on work performed at Luleå University of Technology in cooperation with Mefos, is about measurement of pulverised coal flow injected into a blast furnace, compensating for some of the usually used coke. Coal is drawn from an injection vessel and transported under pressure with the help of nitrogen gas to a blast furnace. It is blown through pipes to the tuyeres where it is injected into the iron making process.

Irregular coal supply to the furnace has bad influence on the quality of the produced iron so reliable control is needed. In controlling the flow, it is of great importance that the on-line flow measurement is accurate. Enhancing the existing measurement would be beneficial for the quality of the produced iron. Therefore new means of blast furnace process surveillance and flow measurement, using cameras and image processing, are studied. The idea behind camera surveillance is also beneficial for estimation of other process parameters.

The main goal is obtaining relevant information from image data in order to estimate the pulverised coal flow. Methods for achieving this are investigated and discussed. A comparison to old measurement data is made. Also validation of data retrieved with the help of image processing is mentioned.

It has been shown that video monitoring in conjunction with image processing is a feasible option when it comes to coal flow estimation. The images include potential information for other purposes like determining the temperature of the flame and how well the coal is distributed inside the blast furnace. This would solve some of the problems and eliminate obstacles caused by the nature of the steel making process.

Preface

People have always asked us: Why study automatic control? The real question is: Why not? There are not many fields that affect our modern life as much as automatic control does, of course mathematics and possibly physics are cornerstones in any nutritious study. They are hard to compete with. Applied science in all its forms is the way to go to enhance products and tools that are essential in today's society. The achievements in the field of automatic control are surrounding us in our everyday lives, no matter if we like it or not. A lot of things out there are already done, many more are waiting to be done. There is also a lot of fine tuning to take care of, which is sometimes even more challenging. We wanted to be a part of this evolving development. We want to thank Anders Grennberg, without him we would not be closing loops these days.

This work is a part of a bigger project with involvement from the industrial and research world, backed up by PROSA - Centre for Process and System Automation[1]. Our master thesis was carried out at the Department of Computer Science and Electrical Engineering, Control Engineering Group at Luleå University of Technology[2] in cooperation with Mefos[3]. The work you hold in your hands is brought to you by two human beings, but is a result of many more human participants. People without whose knowledge and willingness to help, you would not be able to read this report.

During the time we spent on this research we learned to know several people with different backgrounds from different companies, gained more understanding of the complicated coal injection process in a blast furnace, and improved our skills in image processing.

We had great help from our examiner Professor Alexander Medvedev and our supervisor Ph. D. Olov Marklund, both at present working for the Department of Computer Science and Electrical Engineering at Luleå University of Technology. Thank you for offering us a part of your valuable time. We would also like to thank Andreas Johansson, Wolfgang Birk and other researchers at the Control Engineering Group. Roland Lindfors at the AV-centre. Per Mäkikaltio and others at the Division of Industrial Electronics and Robotics. Krister Engberg at the Division of Signal Processing for putting up with us. The system administrators, Mattias Pantzare and Jonas Stahre for their indispensable help. All working at Luleå University of Technology. The Free Software Foundation[4] offering the world the best they can achieve, without them we would be dependent on commercial software, except for MATLAB where we had no time to write the needed toolbox for Octave[5]. Not to forget the helpful people at Mefos, LKAB, Securitas and Björn Olsson at SSAB. Re-Tek members for keeping up the spirit of being atrocious and taking the computers we borrowed before we finished the project. El-Tek members

[1]PROSA's home page. URL: http://www.sm.luth.se/csee/prosa/html/

[2]Department of Computer Science and Electrical Engineering's home page. URL: http://www.sm.luth.se/

[3]Mefos' home page. URL: http://www.mefos.se/

[4]Free Software Foundation's home page. URL: http://www.fsf.org/

[5]Octave's home page. URL: http://www.che.wisc.edu/octave/octave.html

for making it possible to buy provisions during the time we spent writing this report. Last but not least, we want to thank our friends for their psychological support.

Thank you all, you made us do it.

Contents

CHAPTER 1

Introduction

Heavy industries are the backbone of our society, any improvements in this area mean indirectly a better standard of living. Steel and iron production is one of these industries. Steel making has evolved dramatically since mankind learned how to produce it. Yet there is still a lot to do because the process itself is quite complicated and not fully understood. New technology has contributed in many ways to improve the steel making procedure, where involvement of people with different backgrounds and academic knowledge is essential.

In existing blast furnaces there are many problems, which remain unsolved despite many years of thorough research. New improvements and breakthroughs are made every day, but there will always be more work to be done due to the sophisticated process nature. Efficiency, quality, environmental issues and cost reduction requirements are the main objectives. The fuel used in the furnace is one of the targets. Changing the kind of fuel used has shown very good results. Traditionally coke is used. Many other alternative fuels [**10**] have been tested, such as pulverised coal, natural gas, oil but also waste materials. The future supply of coke [**1**] is another problem that might lead to steadily increasing prices. Pulverised coal has become a good alternative. It is 30-40% cheaper and more environmentally friendly [**12**] than coke. Using pulverised coal resulted in a 40% saving in coke requirements at British Steel, Scunthorpe works [**11**], [**13**]. In addition, pulverised coal has a quicker impact on the reaction in the active zone of the furnace.

Beside choosing an alternative fuel, steelmakers need a better overview of the process. Controlling the product quality relies on identifying the process parameters from a metallurgical point of view and how well the process is controlled. Controlling the process, beside unidentified process parameters, runs into problems related to flow measurement, temperature measurement and fuel distribution in the blast furnace which are hard to deal with using old-fashion techniques because of the high process complexity and the very demanding environment.

Quick development in computer hardware has opened new perspectives and possibilities. At present it is an easy task to process a large amount of data to extract useful information in order to control and supervise the steel production in a blast furnace. One way to do this is the use of cameras pointed to the pulverised coal outlet from the tuyeres into the furnace. Camera images can be analysed in order to determine different important process parameters. The goal is to calculate high quality parameters that reflect what happens in the furnace. This will make life easier for metallurgical and automatic control people.

A prestudy [**2**] has shown that there is a significant relation between the pulverised coal mass flow estimation and the size of the coal plume in the analysed video recorded series of images. The recording was done with a black and white camera. Deeper investigation is required to verify the results and find algorithms for calculation of the coal plume volume and coal flow estimation, but also temperature and coal powder distribution. It is also interesting to study the result obtained with a colour camera in order to use several independent estimation channels. In this report we will focus on the first part, i.e. coal flow, but our results will hopefully be useful for the other targets too.

CHAPTER 2

Process Description

We had an opportunity to work on LKAB's experimental blast furnace at Mefos [**17**], where we had a setup of cameras and a possibility to collect needed data. In this chapter we will briefly describe the different parts of the plant and the coal injection part of the process.

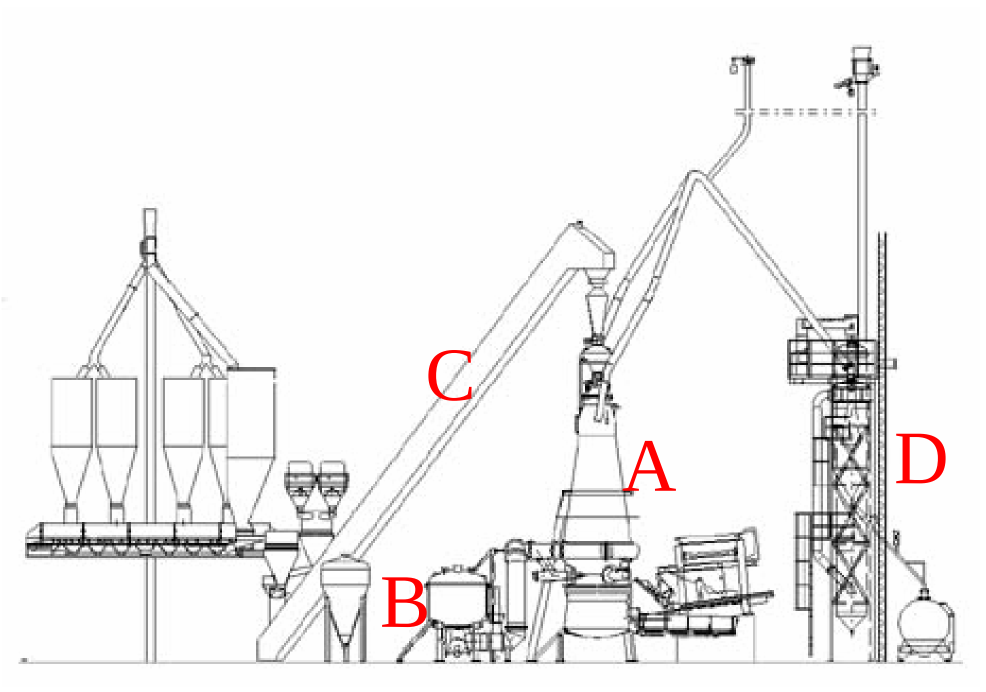

FIGURE 2.0.1. A schematic overview of the plant at Mefos.

2.1. The Blast Furnace

The blast furnace at Mefos is marked with an "A" in Figure 2.0.1. A picture of the actual installation is in Figure 2.1.1. It has three tuyeres and a diameter at the tuyere level of 1.2 m. The working volume is 8.2 m^3. The hot blast is produced in pebble heaters, capable of supplying 1300 °C of blast temperature. The furnace is designed for operating with a top pressure of 1.5 bar. It has a bell-type charging system without movable armour. The coal injection system, see "B" in Figure 2.0.1, features individual control of coal flow for each tuyere. Gas cleaning system, part "D" of Figure 2.0.1, consists of dust catcher and electrostatic precipitator. Material is transported to the top of the blast furnace through "C" as shown in Figure 2.0.1. A tapping machine with drill and mud gun is installed. The blast furnace is well equipped with sensors and measuring devices, and an advanced system for process control. Probes for taking material samples from the furnace during operation are being developed.

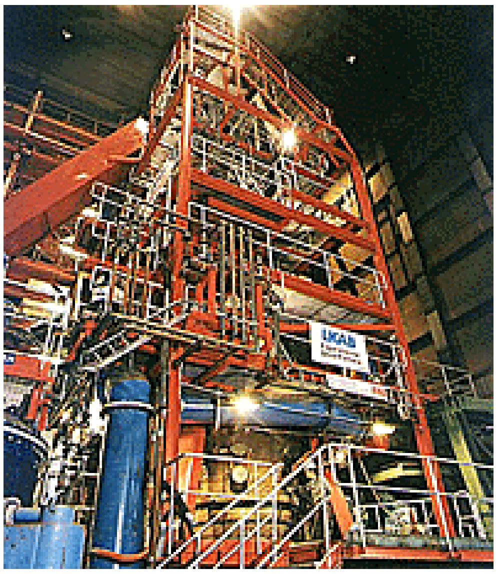

FIGURE 2.1.1. The blast furnace body.

LKAB use the furnace primarily for development of the next generation of blast furnace pellets. The furnace performance shows that it is a good tool for other development projects. An important area is recycling of waste oxides. Injection of waste oxides is another research area as well as injection of slag formers. The interesting parts of the plant are presented in Figure 2.1.2.

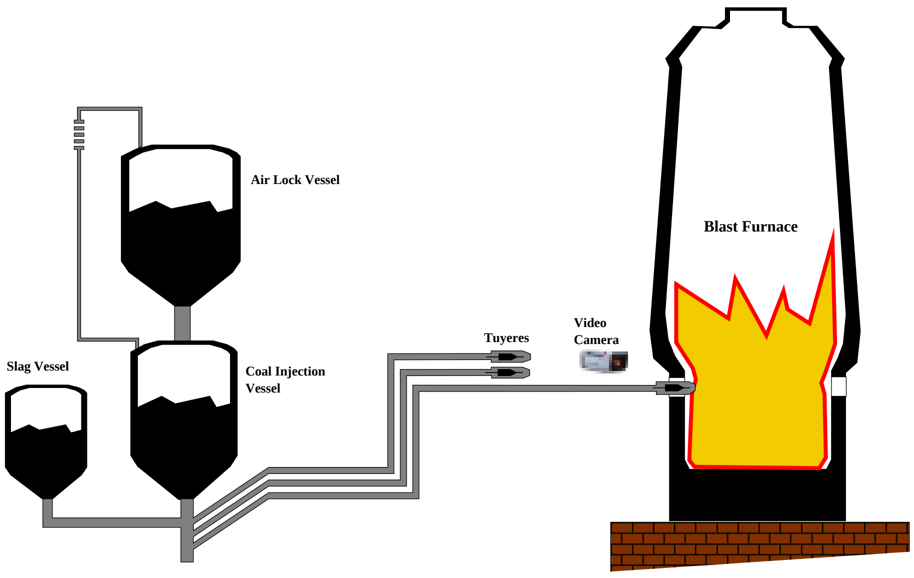

FIGURE 2.1.2. The most relevant parts, for this project, of the experimental blast furnace at Mefos.

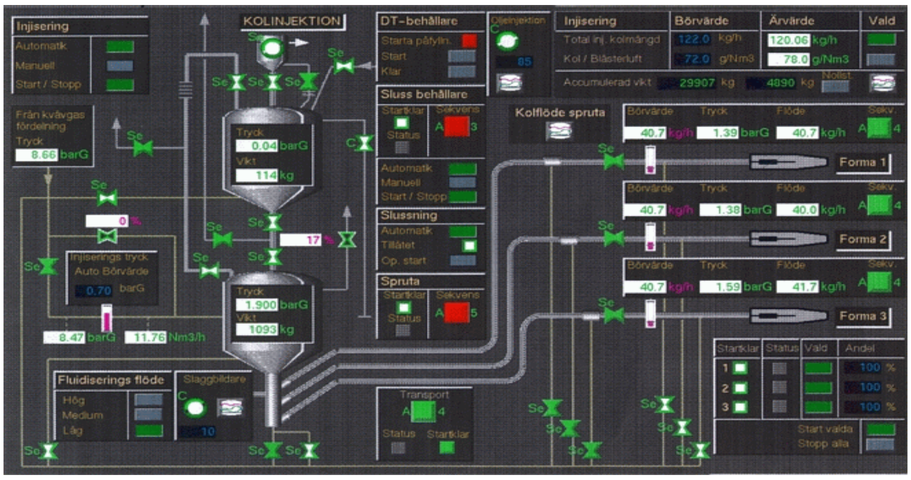

FIGURE 2.2.1. Control screen for coal injection, at Mefos.

2.2. Coal Injection

The coal injection arrangement, Figure 2.2.1, consists of two coal vessels and three pipes each ending with a tuyere. The three tuyeres are evenly spaced around the blast furnace, as shown in Figure 2.2.2.

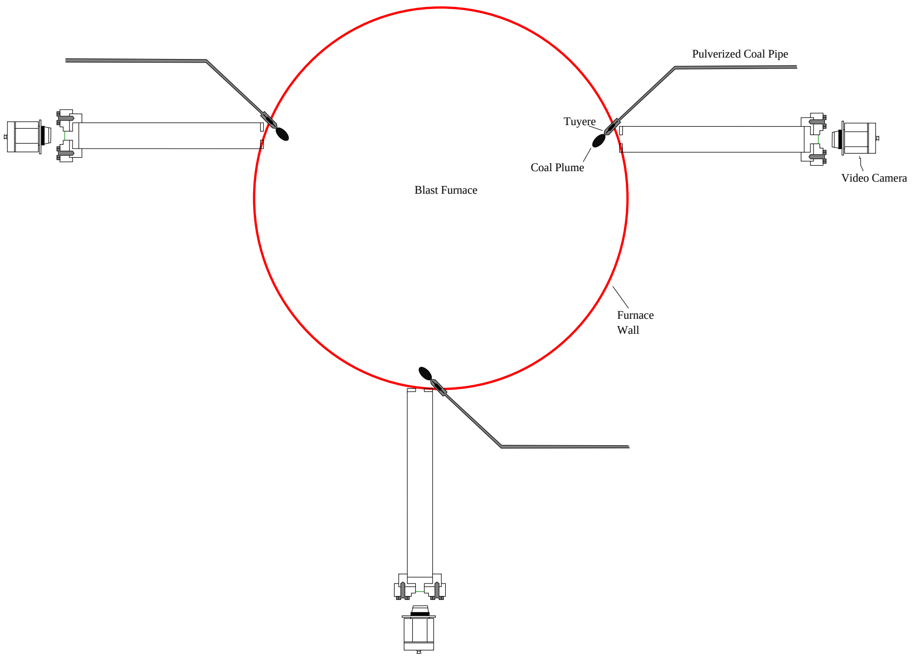

FIGURE 2.2.2. The three tuyeres are surrounding the blast furnace with the surveillance cameras supporting framework.

Looking again at Figure 2.1.2. The upper vessel, the one that is filled with coal when needed, works as an airlock vessel used to pressurise the coal vessel below. From the lower vessel, called the injection vessel, coal is divided and distributed under pressure through pipes to the tuyeres in the blast furnace with the help of nitrogen, which serves as a carrier medium. The left vessel is used to inject slag when desired. A big problem is determining the behaviour of the coal particles travelling through the pipes. That is because of the various size of the particles, turbulence effects in the pipes and pipes' characteristics. Coal particles can clog in a pipe, which can disturb the process before being discovered. Another problem is leakage of the carrier gas. Solution for the latter is proposed in [**6**].

2.3. Current Control

The existing control of the pulverised coal flow to the blast furnace is based on a continuous on-line measurement of the coal flow itself. Although this is true, it is not the whole truth. It has been shown that the flow measurement device is not very accurate, that is why the current control is dependent on a weight measurement of the injection vessel.

2.3.1. Sensors. Mainly we can talk about three flow measurement devices, every one of them connected to pipes transporting pulverised coal to the tuyeres. The devices used are Ramsey DMK 270 industrial mass flow rate and velocity measuring instruments for non homogeneous media [**16**]. Internally the device consists of a solids concentration sensor and a velocity sensor with two measurement points separated by a distance S, based on the capacitive measuring principle. The particle stream is measured in two points which the velocity transmitter correlates to find the closest similarity between them. From this correlation function, the transit time T from point one to point two can be determined. In the solid concentration sensor the change in capacitance is proportional to the solids concentration, this voltage signal is transformed into a frequency signal and is Pulse Frequency Modulated (PFM).

The flow rate Q is given by $Q = C \cdot V \cdot A_{sensor}$, where C is the concentration of the medium, V its velocity and A_{sensor} is the sensor cross-section area and is calculated with $A_{sensor} = \frac{d^2_{sensor} \cdot \pi}{4}$, where d_{sensor} is the sensor diameter.

The concentration $C = \frac{K_a}{10} \cdot (f_{PFM} - f_{PFM_0}) \cdot K$, where K_a is an adaption factor to concentration sensor, f_{PFM} is the measured frequency of PFM concentration signal, f_{PFM_0} is the frequency of PFM signal at concentration zero and K is a calibration factor. Finally the velocity is calculated with the well known formula $V = \frac{S}{T}$.

Not to forget that the both vessels are equipped with weight gauges and pressure meters. Other important sensors are the pressure measurement devices in the coal injection pipes.

2.3.2. Controllers. Figure 2.3.1 is a schematic overview of the main controllers. Because the flowmeter is not reliable, the on-line flow measurement is multiplied by a correction factor calculated according to the injection vessel weight loss deviation, during a certain period of time. See Figure 2.3.2 for details. Doing so the idea of on-line measurement is lost, in a short term perspective, while it is relatively accurate considering a longer period of time. The corrected flow measurement itself is the output of a PI-controller using 1 as its setup value and feedback with the flowmeters to coal vessel weight ratio. Before dividing the flow measurement by the vessel weight both signals are windowed with a window length of 10 minutes before performing the division. This is done because the scale used in the vessel has a limited sensitivity and a big error margin, if compared to the flow measurement during a short time.

The coal injection is controlled with three PID-controllers, one for each tuyere. An operator is supposed to feed the system with the desired amount of coal flow needed in the furnace, the amount is divided by three and the result serves as a setup value for each of the controllers. The output from the PI-controller is used as

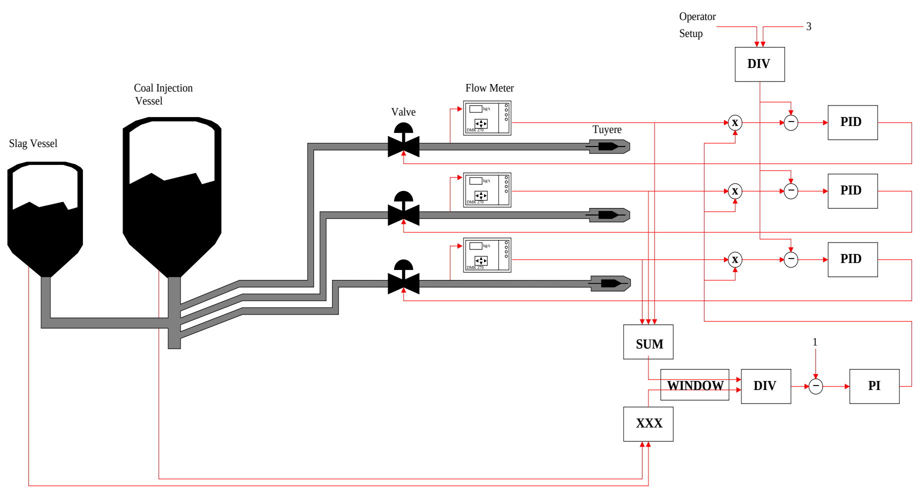

FIGURE 2.3.1. Coal powder injection control.

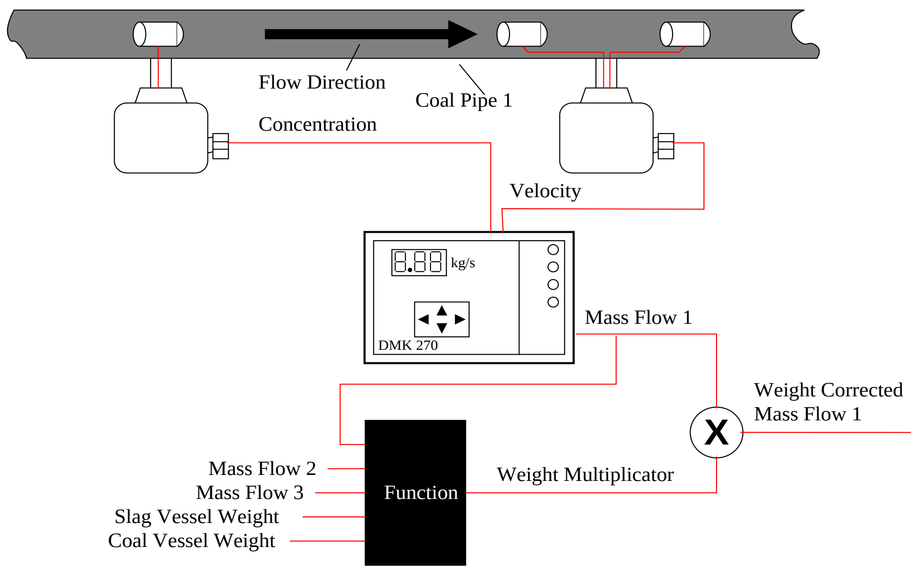

FIGURE 2.3.2. A principle scheme for pulverised coal mass flow calculation.

feedback. The control signal from each of the PID-controllers is used to control a valve placed before the flowmeter on each pipe. A control based on these terms can not be perfect having in mind the bad quality of the resulting measured/calculated signals. Depending on how the multiplicator changes, the control signal will behave differently. We will show later in Chapter 4.1 that some control signals have a strange behaviour.

2.4. Video Surveillance

The conditions surrounding the steel making procedure are rather rough. The very high temperature of the flame and the high brightness from inside the blast furnace make life hard for those who want to control or study this process. The existing cameras at Mefos can not handle the incoming high light intensity and they need to be protected from the heat. A damping filter has to be employed to make the video picture viewable. The filter itself is a dark green piece of thick glass that is placed a bit away from the camera lens. The cameras themselves are mounted about two meters from the outer wall of the blast furnace and are built-in inside a protecting cover. The light from inside the furnace is led to the cameras through peek holes in the wall near each tuyere via protecting pipes.

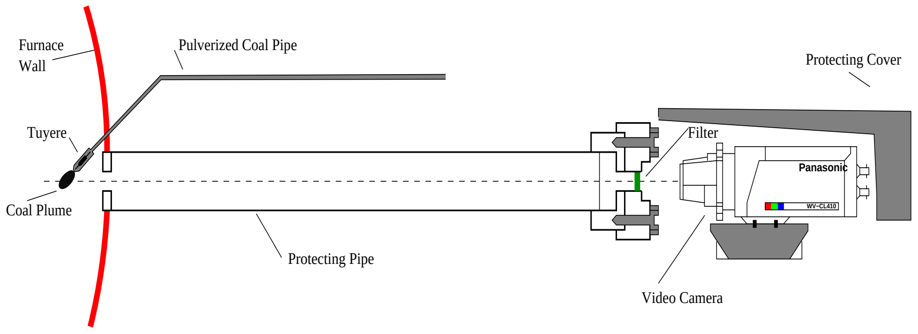

FIGURE 2.4.1. The video camera setup.

For a full comprehension of the whole video camera apparatus, Figure 2.4.1 might be helpful for the devoured readers. On its way to the lens light passes the previously mentioned glass filter. The characteristics of this filter have not been examined in great detail but having a closer look at the three colour buffers shows, for the human eye, that the red and in particular the green light pass the filter almost unaffected while the blue light is filtered out to the extent that the blue buffer becomes nearly useless, as discussed in Chapter 5. It is therefore desired to solve the filtering problem. We had the possibility to use transparent glass instead of the green one, which we believed would leave all the three colour buffers unspoilt. By doing this we risked introducing overexposure to the video surveillance system. Possible solutions will be discussed later in this report.

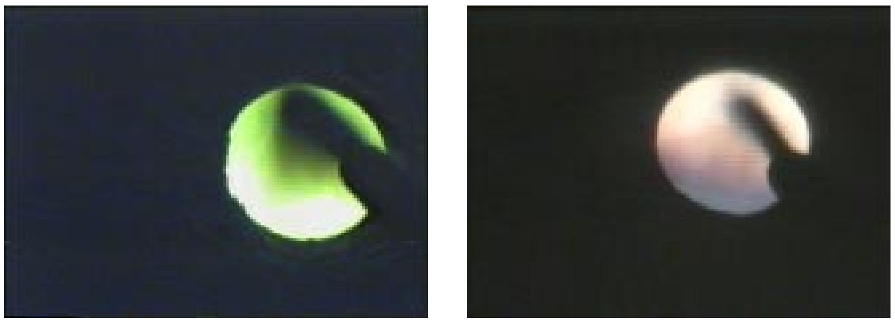

(a) With green glass. (b) With transparent glass.

FIGURE 2.4.2. Sample images taken with green glass as filter and with transparent glass.

An example of what is seen with the help of the cameras is in Figure 2.4.2, where the mouth of the tuyere is seen together with a dark, elliptic shaped cloud, the pulverised coal injected inside the furnace.

CHAPTER 3

Collecting Data

Doing a project of this nature needs of course collaboration with the industry in order to improve things. Simply there is a need of being at the field for investigating possible ways to get across suitable data to kick-off the project. People working at the plant know how to run it and how it behaves. Collecting data does not only mean pure data measurements, it also includes collecting the knowledge possessed by the plant workers. Every detail is important, every worker has something to tell that we probably need to know. The knowledge we gained from people in the field is spread all over the report. Below we are dealing mostly with measurement data collection.

3.1. Available Signals and Equipment

To start with, we will shortly discuss which signals were available to us for further study. After an exhaustive investigation of the process and the parameters that were available and examining the signal collecting equipment we finally concluded what had to be done. It was obvious right from the start that the coal flow signals were of importance for this project. Also the nitrogen pressure in the pipes leading the pulverised coal to the blast furnace was thought to be of interest. Further some other signals were considered in case they would later show to be significant for the study of the coal powder flow. For convenience Table 1 with available signals is attached. Of course there were many other signals available but we did not think that they were of interest.

Nr.	Connection	Internal Signal Tag	Signal Description	Range
1	205	31PI101	Pressure, inj. pipe 1	0-16 bar
2	207	31PI102	Pressure, inj. pipe 2	0-16 bar
3	209	31PI103	Pressure, inj. pipe 3	0-16 bar
4	298	31FV138	Control sig., pipe 1	0-100%
5	300	31FV139	Control sig., pipe 2	0-100%
6	302	31FV140	Control sig., pipe 3	0-100%
7	029	31FI101	Mass flow, pipe 1	0-41667 g/s
8	031	31FI102	Mass flow, pipe 2	0-41667 g/s
9	033	31FI103	Mass flow, pipe 3	0-41667 g/s
10	237	31PI021	Pressure, inj. vessel	0-20 bar
11	470	31WI001	Weight, inj. vessel	0-3000 kg
12	322	31PI108	Pressure, lock vessel	0-16 bar
13	474	31WI102	Weight, lock vessel	0-3000 kg

TABLE 1. The considered signals and their description.

Unfortunately the collected signals could not be taken straight from Mefos' computer system. The reason for this was simply the deficient capacity of the presently used system. In this case it was necessary to wire a signal collecting equipment into an electrical cabinet, consisting of a National Instrument data acquisition box SCXI-2000 equipped with SCXI-1120, an 8-channel isolation amplifier and SCXI-1100, a 32 channels programmable amplifier with gains. Those modules contained an IO-board and an analogue to digital converter with amplifiers. In total we had two different opportunities to log signals, we did that on three different dates. The 8-channel card was used in the third logging session while the other one was what we had in the first and second session. A portable computer was used to store data with the help of the data collecting programme LabView. This was the best option available although not very favourable, which will be discussed later. The signals in the electrical cabinet were in the range of 4-20 mA, a current circuit connection was employed for its robustness to signal noise, not affecting the plant and its easiness.

Not surprisingly this project also demanded video recordings from the three cameras, beside the previously mentioned signals. These video signals could be found at another electrical cabinet at the plant. Using ordinary video recorders, video signals could be recorded for later usage and investigation.

3.2. Measured Signals

Knowing the situation presented in the previous section and the uncertainty of which signals to collect, a decision was made to collect all of the 13 listed signals considered if possible. This was done during the first data gathering on the 4th of June 1999. Although some problems arose in the blast furnace, data was stored on a laptop and transferred to stationary computers standing in a small image processing lab at Luleå University of Technology, for later consideration. A couple of days later sadly the pressure signal of injection pipe 1 was discovered to be faulty. It was necessary to arrange another signal collecting session, which was eventually done on the 10th of June 1999. This time all signals were fine except for one of the video signals. Apparently we can not have them all! Again there were problems with the furnace process during data gathering time, which later turned out to possibly be related to the equipment used. Although the data acquisition module was thought to be galvanically isolated. Unfortunately it was found that was not the case. Neglecting that fact collected data was analysed. During both those logging sessions we used the same cabling with 250 Ω resistances.

Wanting to verify what was concluded from the data collected in June another trip to Mefos was required. This time, not wanting to be be blamed for disturbing the blast furnace process once again. Another data acquisition card had to be used. The National Instruments signal collecting box turned out to have a card supporting collection of only eight signals at a time, if they were to be isolated. We also changed the cables used and switched to 50 Ω resistances. This was found to be a good solution after an examination of what went wrong with the blast furnace process during the June sessions at Mefos. Of course, a limitation like this meant a risk. An omitted signal could later turn out to be of great importance. We had to concentrate on two of the three tuyeres, specifically pipe 2 and 3. The chosen signals have, looking in Table 1, numbers 2, 3, 5, 6, 8, 9, 10 and 11. Motivation for this choice was that mass flow was wanted together with both the control signal and pressure signal. Weight of the injection vessel as well as the pressure inside it were also taken into consideration on the expense of the control, pressure and flow signals for tuyere 1. Control, pressure and flow signals in pipes 2 and 3 were thought to be sufficient regarding the small number of signals that could be gathered using the available equipment. The main reason for this logging session was to record a new video signal of the injection without using a green glass filter, instead we changed the glass in front of the camera in pipe 2 to a transparent one. The glass in front of the other camera, pipe 3, remained unchanged. Bad luck and possible wiring problems resulted in a missed signal, this time it was the coal injection vessel weight. A summary list can be found in Table 2. Other activities at the plant linked to our work can be found in Table 3.

Occasion	Date	Time Duration	Collected Signals	Tuyeres Recorded
1	999-06-04	17:54:08-18:47:23	2-13	1, 2, 3
2	999-06-10	12:45:46-14:49:08	1-13	1, 2
3	999-11-18	13:24:34-15:04:24	2, 3, 5, 6, 8, 9, 10	2, 3

TABLE 2. Data collection occasions.

Occasion	Slag $\left[\frac{g}{Nm^3}\right]$	Coal Setup Value $\left[\frac{kg}{h}\right]$	Tapping Time
1	No	130	18:47-18:51
2	20	125	3:04-13:19 14:30-14:36
3	No	125	14:05-14:15

TABLE 3. Activities and setup values during the logging time.

During the third logging session we had an opportunity to disturb the coal flow in one of the pipes. We chose pipe 2. This test series originated from a need of data for an extra validation of achieved results in a different project ran by Ph. D. student Andreas Johansson related to his research in clogging detection in a pressurised system [**6**] at Luleå University of Technology. We refer to this test series as Andreas test. This test is also interesting in our case to see if we can detect the flow changes with image processing. We had two valves which we could close to prevent the coal flow into the furnace. The first valve was located directly after the injection vessel and before the flowmeter, the other valve was placed after the flowmeter; we refer to those as the valve before and the valve after, relative to the flowmeter as illustrated in Figure 3.2.1. We opened and closed the valves repeatedly with different throughput rates. The test duration was limited due to a desire for not affecting the plant or ending up with a plugged pipe. We realised later that the time between the different actions was not far from the limit of being too short, because the flow measurement is very strongly filtered; see Chapter 4.1 for further insight.

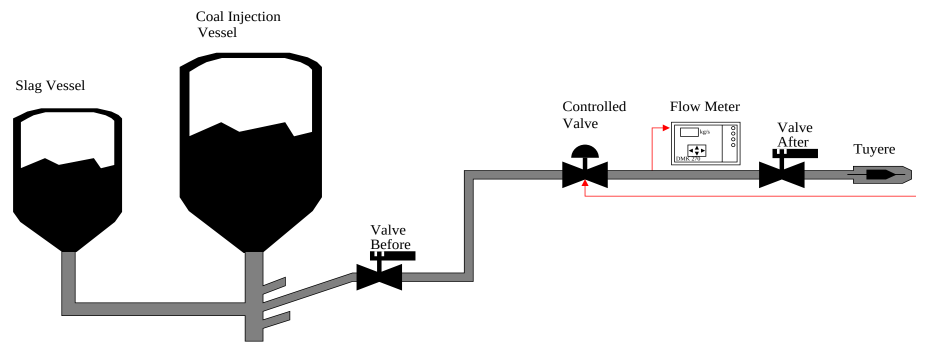

FIGURE 3.2.1. The locations of valves along the injection pipe.

Table 4 shows the actions taken during the test, the valve position we mention is actually the valve handle position and not the real valve opening rate (position) which is most likely non-linear. Notice that the valves were totally opened before and after the test. Other signals as slag vessel weight and its pressure as well as weight correction multiplicator should have been collected, but this was not discovered before it was too late.

Action	Time	Valve placement	Valve position
1	14:23:30	after	1/2 closed
2	14:24:30	after	1/1 opened
3	14:26:00	after	1/1 closed
4	14:27:00	after	1/2 closed
5	14:27:30	after	1/1 opened
6	14:29:00	after	1/2 closed
7	14:31:40	after	1/1 closed
8	14:33:00	after	1/1 opened
9	14:36:00	before	1/2 closed
10	14:36:30	before	1/1 closed
11	14:37:30	before	1/1 opened
12	14:38:00	before	1/2 closed
13	14:39:00	before	3/4 closed
14	14:39:40	before	1/1 closed
15	14:41:00	before	1/1 opened

TABLE 4. Actions and time schedule during Andreas test.

3.3. Video Recording

At the same time as data was collected using the data collecting module a video recording had to be made. This was clearly a sensitive issue to deal with. The time delay between the start of collecting other data and recording the video signals from the cameras had to be determined in some way, because those signals were to be compared during later analysis. The only viable alternative was to start gathering data at a certain point in time, then start the video recording and marking a fixed point in time on the film sequence by manually dimming the light to the cameras for a couple of seconds. That way the time delay was restored later when analysing data. Using a more sophisticated synchronisation method would be a better option if it was not such a lengthy procedure, remembering that the electrical cabinets and the cameras are apart from each other making a complex wiring scheme doomed to fail in such environment, and also having in mind the quite small benefits employing an approach different from the simple solution used.

Video cameras presently installed at Mefos are of the type Panasonic WV-CL 410. These cameras were used at both occasions in June. However in November a decision was made to try another, slightly more advanced camera for filming the injection at tuyere 2. The camera used was also a Panasonic camera from the 400 series. The difference was mainly the larger dynamic range, and employment of a new Panasonic technique known as SuperDynamic. Good reference manuals with the camera specifications could not be found. The necessity of using a more advanced camera occurred to us when trying to record a film sequence without the dark green protecting glass. Operators knew from experience that the existing cameras were not able to handle the intake of very bright light when the protecting glass was removed. Removing the dimming filter, transparent glass was mounted in its place. The new camera used was performing better than the old one but unfortunately it also reached the saturation point due to the extreme brightness of the light from inside the blast furnace.

Another problem discovered during the signal collecting session in November was the dynamic adjustment of the range. This caused changes in the background of the picture depending on the amount of visible coal. When there is a lot of coal the picture is percepted as darker by the camera so it adjusts to a darker picture, when there is no coal the picture is brighter and again the camera adjusts accordingly. As a result of these constant adjustments we get a background for the pulverised coal cloud that is constantly changing. Those changes are not great but can be irksome when, for instance, trying to retrieve information about the temperature of the flame. Problems are in that case caused by the fact that a change in colour does not have to reflect a change in temperature, which seems like a troublesome case to solve. Maybe the easiest way to deal with this problem would be disabling the auto adjustment function in the cameras used.

Further another source of concern is the noise introduced by the poor quality video tapes and the video recorders themselves. Watching a recorded sequence it is apparent for a human observer that unwanted noise is present. Luckily the extent of this phenomenon is limited and it should not affect the outcome of later analysis too much.

All problems discussed are evidently of harm for the quality of images to be analysed. Obviously a higher quality of images is better but it has to be pointed out that their quality is still well above what is needed for image processing to be performed in order to obtain vital information about the blast furnace process.

3.4. Video Digitising

The recorded video signals on the tapes needed to be converted into a usable format in order to process them in a computer. Digitising the video signals was required. It is always hard to choose a computer environment to work with, in our case the choice was easy. Microsoft's Windows family has never been a choice of a serious researcher/engineer and hopefully will never be, specially when she/he deals with automatic control. Free Software is widely available, reliable, supported and sufficient in most cases. We used RTLinux as a platform for digitising the video tapes we recorded. Using an ordinary S-VHS video player, a common PC (old timer) equipped with RTLinux, a Matrox Meteor frame grabber card and a simple grabbing program, see the source code in Appendix B.1, the work was accomplished.

The task here is to convert a full motion video, PAL-signal (Phase Alteration Line) running at 25 frames per second, into single frames stored in a digital format. The first step in the process of converting an analogue signal into a digital representation is sampling. This is accomplished by measuring the value of the analogue signal at regular intervals called samples. These values are then encoded to provide a digital representation of the analogue signal. The power spectral density (PSD) of the flow signals, we have collected, shows that in the worst case a sampling time of two seconds is sufficient. Remember that we are not sampling to control, we are just trying to recreate the flow signal in someway. Two seconds might sound too fast but some of our flow signals have a significant frequency peak caused by bad control. The same frequency peak has been found in the pressure and control signals. See Figure 4.1.3 for a closer look at PSD signals related to pipe 2, taken form the second data collecting occasion, which can be compared to the ones related to pipe 1, also from the second occasion, in Figure 4.1.4. As you can see the peaks in (a), (b) and (c) are below 0,2 Hz, which means according to Nyquist's sampling theorem, that a sampling time of 2,5 seconds ($\frac{1}{0{,}2\cdot 2}$) should be sufficient. Choosing

3 seconds sampling time is kind of adventurous because it will catch up with frequencies up to 0,16 Hz which may result in some aliasing in our case. We assumed that the characteristics, in the collected signals, would be reflected in the data to be extracted from the recorded video signal. Actually the flow measurement device used a couple of seconds data filtering and the control system used at Mefos use a time base of 0,20 - 0,25 seconds.

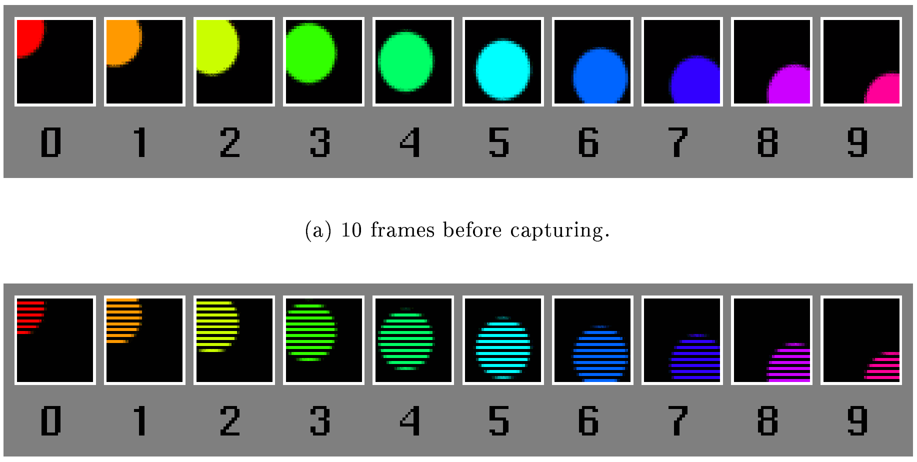

(a) 10 frames before capturing.

(b) 10 captured fields of the frames above.

FIGURE 3.4.1. Interlace principle [**3**].

Video is sampled and displayed such that only half the lines needed to create a picture are scanned at a particular instant in time. A video frame in our case consists of two interlaced fields of 625 lines. Interlace is the manner in which a video picture is composed, scanning alternate lines to produce one field, approximately every 1/50 of a second in PAL. Two fields comprise one video frame. As shown in Figure 3.4.1, if the upper sequence is captured by a conventional video camera the result will be the lower sequence which means that our frame consists of two different fields captured at different times. This is a drawback in digitising analogue video signals that use interlace. We had to separate each captured frame into two fields, but this did not affect our results. A reason for that is: We sampled at a very low rate compared to the field rate and it is not very likely that much of the image, in our case, has changed in 1/50 seconds. Figure 3.4.2 shows how this effect is present in our case.

Another important factor when it comes to digitising is the frame grabber equipment. The used frame grabber card, a PCI Matrox Meteor, should be considered as appropriate in our case. The card could make 24 bpp at $768 \cdot 576$ pixels resolution. This gave us $256 \cdot 256 \cdot 256$ (RGB) colours. At the time this project started the device driver available for the grabber card, for Linux, was not of a very high quality. We were forced, due to some possible hardware limitations, to increase the delay time for the card in order to make the desired resolution mentioned above. This could sometimes lead to unwanted effects, which resulted in grabbing an image combined of two frames, see Figure 3.4.3. We had to accept this bug for the time being, specially because it does not appear so often and could not have a major influence on the total result.

We did not use the real-time functionality in RTLinux for several reasons: The program we wrote for grabbing the video frames gave a good synchronisation (a

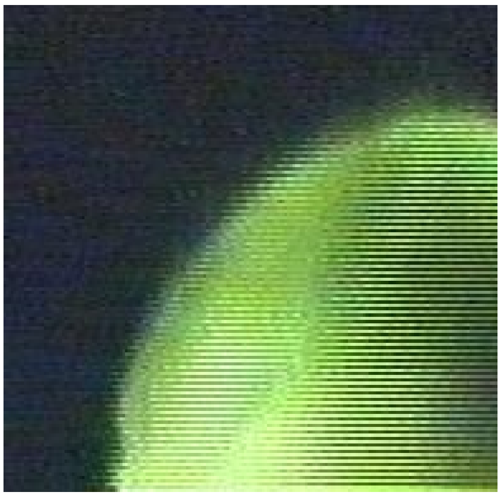

FIGURE 3.4.2. Interlace phenomenon in a sampled frame, from our video recording.

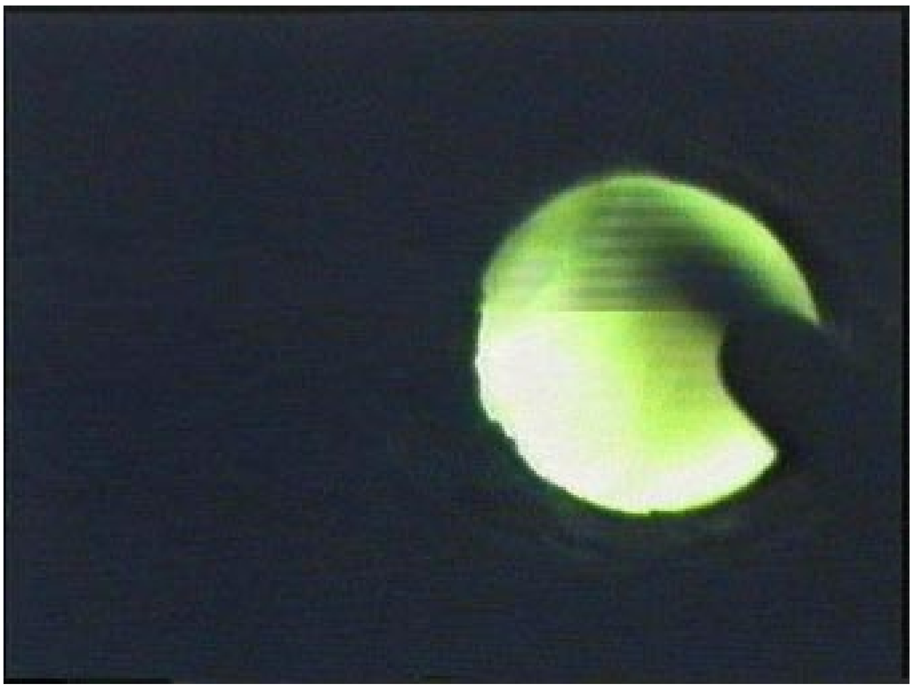

FIGURE 3.4.3. An image composed of two different frames.

couple of milliseconds), the sampling time was 2 seconds so a strict time scheduling was not necessary and we wanted to make the program code for grabbing the frames easier. Bear in mind the data acquisition programme used, LabView, was running on Windows 95 sampling data every second. We have every reason to assume that the sampling was not perfect on the millisecond level.

Because lack of a very good synchronisation signal, as mentioned in Chapter 3.3, to start grabbing the images we had to rely on our extremely good reflex time and start grabbing when the synchronisation signal was visible on a monitor screen attached to our VCR. Any mistakes here will result in a time delay when comparing the logged data with the one extracted from the sampled video recording, which is hopefully much smaller than the overall time delay for the whole system.

A fully operational system based on real-time image processing of the video signal should consider to deal with a short sampling time and enjoy using the real time features in RTLinux.

CHAPTER 4

Data Processing

The collected data is of no use if it is not analysed with a critical eye. Knowing the data characteristics and its limitations is of great help when it is later used in Chapter 7 for validating the extracted flow measurement. Decisions based on the analysed data can then be taken with good accuracy. To make this analysis fast and practical, a small user interface was written in MATLAB. It was given the name Danalyzer from the two words "data" and "analyse" and will be described later in Chapter 4.2.

4.1. Analysis of Signals

Performing the analysis of collected signals it is close at hand to start by looking at the plain signals, comparing their shapes and trends. Trying to find possible similarities which could reveal interconnections and dependencies between the signals is basically the first step.

To start with the pressure signals were viewed. First signal collecting occasion gave us only the last twelve signals according to their numbers in Table 1. As mentioned before the pressure in injection pipe 1 was not stored due to hardware problems. The other two pressure signals looked quite the same, the pressure in injection pipe 3 being slightly higher than the pressure in injection pipe 2. We do not think that should be the case. The level, not considering the fast fluctuations, was quite constant. Then the mass flow for the three pipes was examined. It seemed to be almost the same in all pipes although of course small differences could be noticed. Moving over to the control signals it could be noticed that the control signal for pipe 1 was behaving in a much better way than control signals for pipes 2 and 3. Looking at those signals it is clear that the controllers are not working as they should. Both the control signals 2 and 3 reach their lower bound frequently and are varying quite a lot which indicates bad control. Well, with a risk of being nasty we would say, very bad control. Examine Figure 4.1.1 for clarification. Could this be a result of our non-galvanically isolated data acquisition equipment? A comparison between the control signals from the first and the second data collecting occasions, which we carried out using the same cabling, shows that the control signals do not saturate as often as the one in Figure 4.1.1 does. This makes us conclude that we are not responsible for the bad control, something else went haywire. The controller for pipe 1 functions somewhat better at that given time. Pressure as well as weight of the lock vessel remain constant for the whole time period. For the injection vessel pressure we notice a sinusoidal looking curve with a diminishing amplitude, whereas its weight is steadily falling because coal powder is persistently drawn from it and transferred to the blast furnace and no refillment of the coal vessel has taken place during logging time. The constant negative slope of the signal suggests an even supply of coal to the blast furnace.

The second time we went to Mefos to collect signals we managed to get all thirteen of them i.e. the same twelve as before and also the pressure in injection pipe 1. Pressure signals for the three pipes look very much the same and there is nothing distinctive about them except for the sudden variations seen throughout a

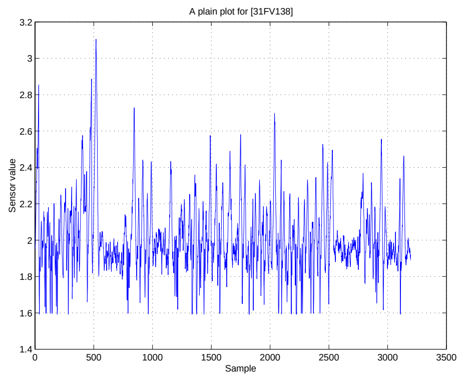

(a) Pipe 1.

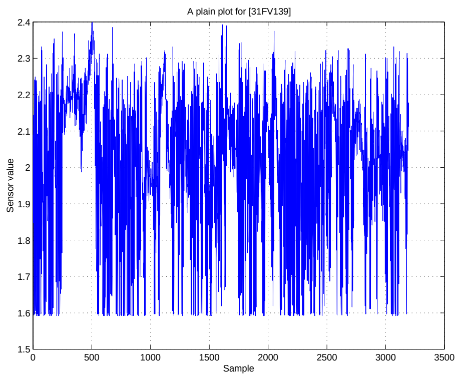

(b) Pipe 2.

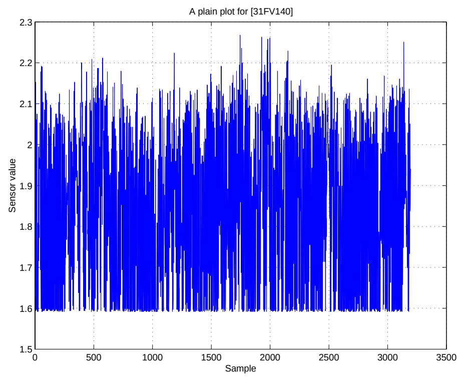

(c) Pipe 3.

FIGURE 4.1.1. Control signals, first data logging occasion. X-axis is samples taken 1 per second and Y-axis is sensor value in Volts.

section in the first part of the data. This is not as obvious in the mass flow signals except for the flow signal for pipe 3. Actually it is hard to tell anything decisive studying the mass flow in pipes 2 and 3. Possibly the flow is slightly higher in the first part of the data. The control signals are weird looking things which have very little in common. Control signal for pipe 1 is following a constant line with quick, high variations. In control signal 2 we can discern that the signal drops after a while which resembles a little the behaviour of control signal 3. In the last mentioned signal again clear deviation from normal behaviour appears in the beginning. Lastly looking at the injection vessel and air lock vessel signals it is clear that something happens exactly the same time as seen in the other signals.

The strange behaviour in the beginning has been shown to be caused by tapping of iron during logging time as stated in Table 3. Although the time does not exactly match there is no indication that it could be caused by anything else. The first tapping is visible in all the signals but the second one appears only in the control signal of pipe 2. It has nothing to do with the duration of the tapping, because the effect on the signals is visible during the whole tapping time. What happens in the blast furnace during the tapping is a very interesting topic to look into.

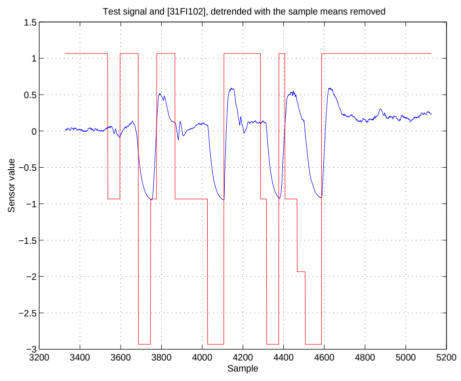

(a) Flow signal, compared to valve position.

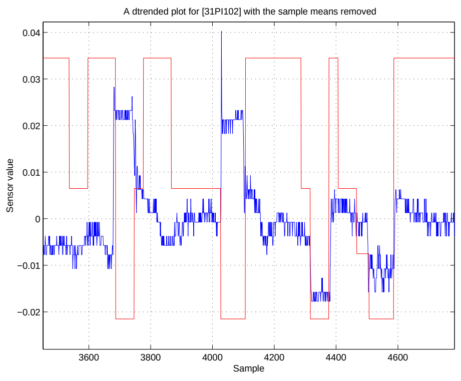

(b) Pressure signal, compared to valve position.

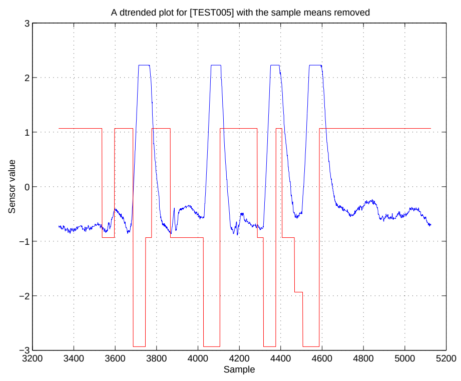

(c) Control signal, compared to valve position.

FIGURE 4.1.2. Measured signals in pipe 2 (blue) compared to valve position (red) during Andreas test. X-axis is samples taken 1 per second and Y-axis is sensor value in Volts.

During the November visit to Mefos only eight signals were collected due to the previously mentioned hardware limitations. One of these signals turned out to be of no use, namely the injection vessel weight signal. Pressure in the vessel seems to be relatively constant. Now looking at the other signals we have to keep in mind that we choked the pulverised coal flow for injection pipe 2 in Andreas test, as we mentioned in Chapter 3.2. Strangling the flow could only be done for short periods of time not to block pipe 2 permanently, needing a serious intervention in the system. Not very surprisingly inspecting the flow signal 2 we can unambiguously see distinct changes in the flow, as Figure 4.1.2-(a) clearly shows. A very interesting thing is the delay in the flow measurement signal, it seems to be caused by some filter; this made us start scratching our heads. Later, this discovery will be treated in Chapter 4.1.1.

Another interesting observation is that the flow is not really affected until a valve is totally opened or totally closed and we have an overshoot when a valve is totally opened. A possible reason is that the valves have a non-linear characteristics and that, as shown below, the flow can be kept as long as the pressure is constant.

A shame is that we never let the flow measurement settle or saturate before we changed the valve position. The pressure signal in pipe 2 did also respond to our test, strangling of the pipe reveals itself by an increment/decrement in pressure. As shown in Figure 4.1.2-(b) the pressure increases each time the valve after the flowmeter is closed and decreases each time the valve before the flowmeter is closed. It seems that the pressure in the pipe can be kept constant when a valve is half closed.

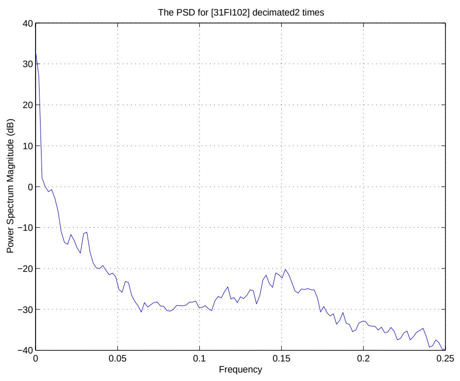

(a) Mass flow.

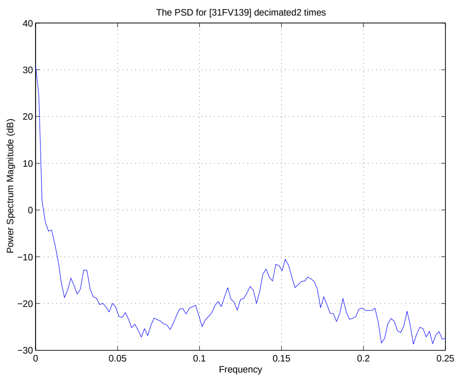

(b) Control.

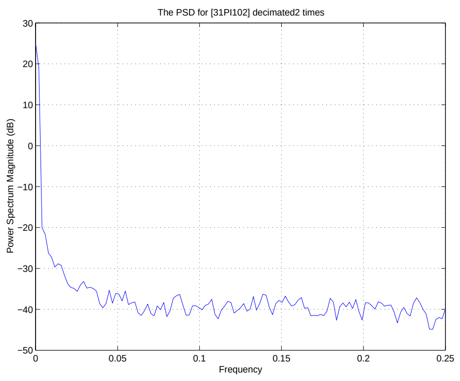

(c) Pressure.

Figure 4.1.3. PSD plots for different measurements in pipe 2, second occasion. Frequency is in Hz.

good look at the control signal of pipe 2, presented in Figure 4.1.2-(c) ensures us about a reaction from the controller. The response time is about 30 seconds. Sometimes we were about to reopen the valve before the controller hits its upper limit. The more important thing is that the control signal increases when the valve is closed, which is an indication of a functioning controller. The controller's feedback, see Chapter 2.3 for further information, is a reason for the bad response time; unless Mefos' engineers have designed it that way. That proves that at least there is a reaction from the flowmeter when the coal flow to the furnace is drastically reduced. What can be considered as strange is that looking at the pressure, control and flow signals for pipe 3 there are no changes that could be directly connected to the changes in the flow for pipe 2. Since the coal leaves the injection vessel and is then divided in three flows one could conclude that smaller flow in one of the pipes would mean more coal in the remaining pipes if the total flow was to be the same. Here we can deduce that either the total flow decreased or that the flowmeters do not work very well.

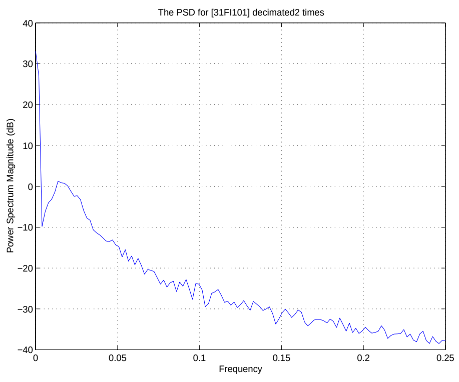

(a) Mass flow.

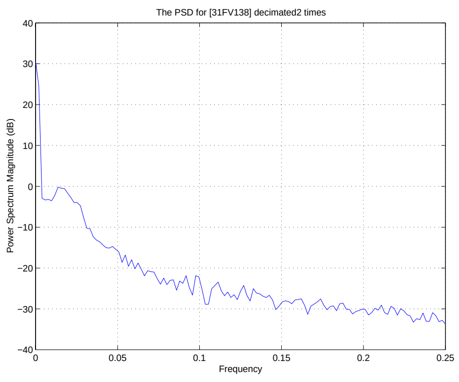

(b) Control.

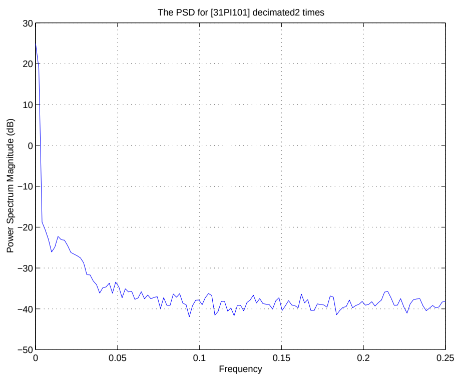

(c) Pressure.

FIGURE 4.1.4. PSD plots for different measurements in pipe 1, second occasion. Frequency is in Hz.

Next step in the study of the collected signals was to try different things, like for example addition, subtraction and other such operation on the different signals. One of the more interesting things tried here was frequency analysis. Frequency contents of our signals were analysed using Danalyzer, just as all of the above analysis to make life simpler and save some time. Studying signals collected on the 4th of June, we found the same dominant frequency for pipe 2 and 3 in control and flow signals, as shown in Figure 4.1.3 for pipe 2. This could point to poor control affecting the flow and making it fluctuate or the opposite, if we assume that the controllers are the same in all the pipes but the flow measurement device behaves badly in different ways. For our purposes though this was an excellent opportunity to check if the same frequency could be found in the processed images. This matter will be investigated in Chapter 7.2, where all the data extraction is performed and thoroughly discussed. We could not identify such control problems for pipe 1, see

Figure 4.1.4, nor could they be found in the signals collected later, which should not be misinterpreted as the control signal being unsurpassed.

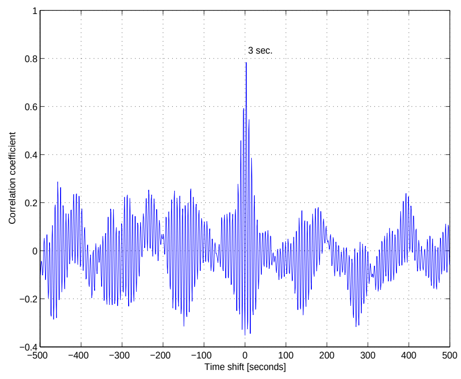

(a) Control-pressure, first logging.

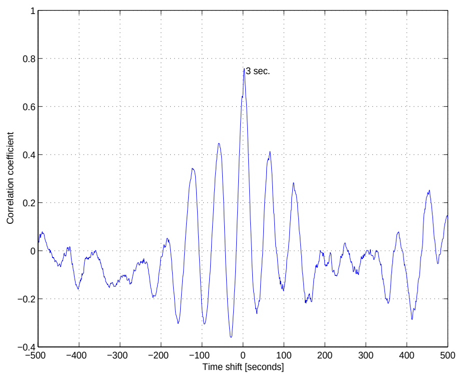

(b) Control-pressure, third logging.

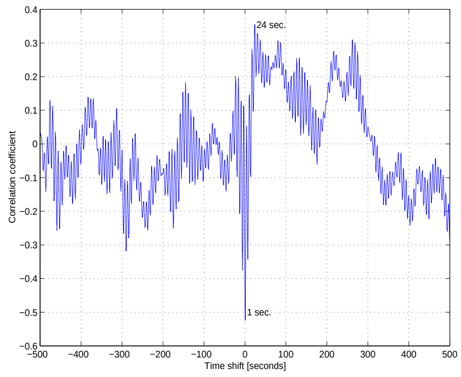

(c) Control-flow, first logging.

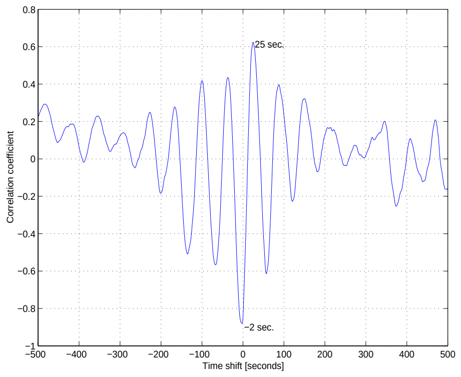

(d) Control-flow, third logging.

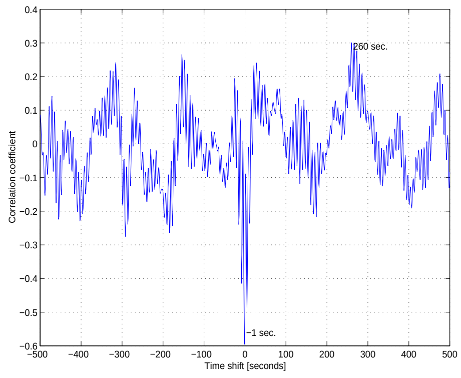

(e) Pressure-flow, first logging.

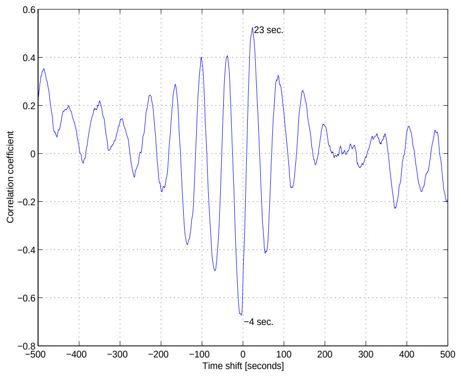

(f) Pressure-flow, third logging.

FIGURE 4.1.5. Correlation between pressure, flow and control signals for the first and third collected data.

By looking at the correlation between different signals, we can see how hard they are coupled and see if there exist any delays. Figure 4.1.5 shows clear correlation between the control and pressure signals. The control signal does not follow the flow signal as well as the pressure does. This indicates that either the control is bad or there is something else beside the flow signal that affects the control signal (which we will see is true here) or both. Almost the same correlation is found between the pressure and the flow signals. The same figure shows delays between the different signals. Notice that the the correlation plots are different if you compare those from the first nd the last occasion, there is a clear frequency present in the Figure 4.1.5-(a) , (c) and (e). It is most likely the frequency we have pointed out earlier, that we call “Mefos carrier-frequency”. Beside the difference in the frequency the delays seem to be pretty much the same in both the first and third data collection. The pressure is very dependent on the control signal with a delay of 3 seconds. In the control-flow correlation we see the clear feedback effect, represented as a negative correlation with a very short delay and the positive correlation with a flow signal following the control signal after a delay of about 25 seconds. Notice also that the negative correlation in the third signal logging is much stronger than the one in the first one, implying a stronger feedback coupling. The pressure-flow correlation plots are very much alike the control-flow correlation plots, with almost the same delays translated by about -2 seconds which confirms what we saw in the control-pressure and control-flow plots.

Having just these signals to study, it is hard to draw further conclusions. They were mainly collected in order to, at a later stage, be compared to data extracted from recorded film sequences. Thus, just as means to verify our sequitures from image processing of the video.

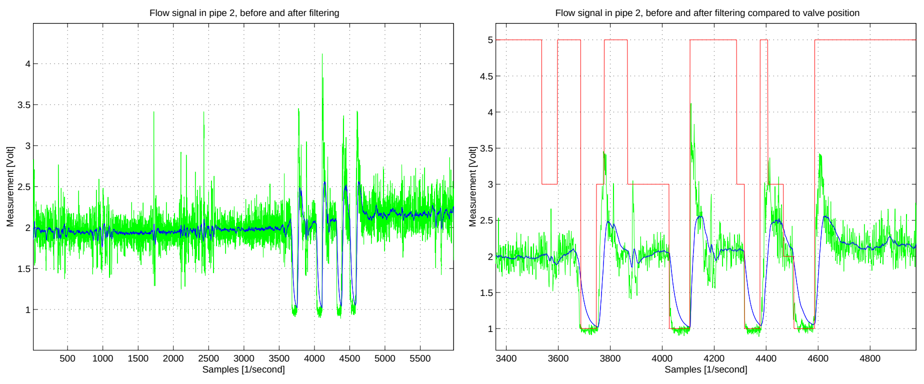

(a) Filtered and unfiltered signal.

(b) Filtered, unfiltered and valve position signals.

FIGURE 4.1.6. Comparison between the filtered flow signal (green), unfiltered flow signal (blue) and the valve position signal (red).

4.1.1. Filter Identification. We saw earlier that the flow measurement did not respond in the way we expected it to do when applying Andreas test. Because we had no access to documentation regarding the flowmeter and the control system in general, at the time we ran into this, we started to investigate the case. A filter was a good way to start in. Connecting a filter to a measurement device is quite common. A possible filter could be: $H(z) = \frac{z\cdot(1-e^{\frac{-1}{22.3679}})}{z-e^{\frac{-1}{22.3679}}}$, obtained by identification.

Inverting the filter and filtering the flow measurement with it should hopefully recreate the supposed original signal. Figure 4.1.6-(a) hows how the filtered signal is related to the original signal and Figure 4.1.6-(b) shows how this fits with the valve position, after zooming on the interesting parts. A further knowledge of the control system has shown that, as mentioned in Chapter 2.3, the feedback signal sent to the controller is not the pure flow measurement we have examined here. Having a look in the user manual for the flowmeter the filters are integrated in the sub-measurement used in the device in order to calculate the flow. For our knowledge the measurement device can not be separated into a flow measurement and a filter.

4.2. Danalyzer

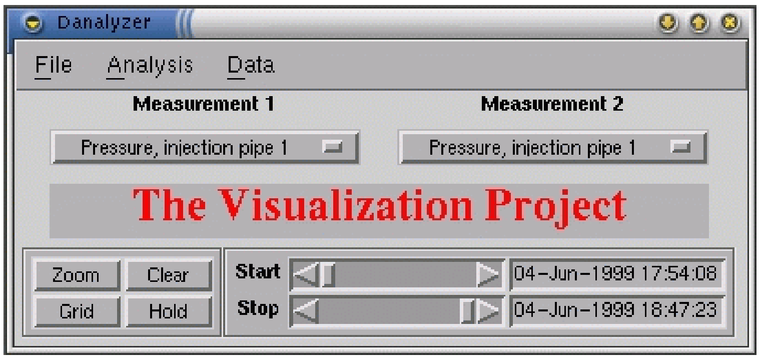

Measurement 1: Pressure, injection pipe 1
Measurement 2: Pressure, injection pipe 1
Start: 04-Jun-1999 17:54:08
Stop: 04-Jun-1999 18:47:23

FIGURE 4.2.1. A screenshot of Danalyzer.

A tool to simplify the routine work in MATLAB had to be developed. We found a tool called Danalyzer[1] that was developed during another project [4] at Luleå University of Technology. Danalyzer was in its early development stage, version 0,1, and needed some work to make it suitable for our needs. After further development we reached what we called version 0,2. A screenshot is in Figure 4.2.1. The Danalyzer essence is its portability and the ability to use for different purposes whenever there are signals involved that need to be analysed. Danalyzer should combine ease of use with functionality and eliminate the tedious work to produce needed plots and perform data analysis.

Danalyzer today is capable of viewing and manipulating data in different ways, the main features are:

- Viewing of signals.
- Browsing through the signals to view specific parts of them.
- Several plots on one window.
- Multiple windows with different plots simultaneously.
- Analysis: FFT, PSD, removal of trends.
- Adding and subtracting signals.
- Decimation of the signals.
- Simplicity in creating data files.
- Possibility of zooming and gridding.
- Loading of signal sets.

[1]Dnalyzer files, version 0,1. URL: http://mir.campus.luth.se/washers/work/danalyzer/

CHAPTER 5

Image Processing

In order to be able to evoke any useful information from the images we have sampled, we need to know more about them. A need for a close examination of the images general properties is as important as the images themselves. As we mentioned before we used two different types of glass as filters during the video recording. We also used two different types of cameras. This makes the comparison we made here below not as bulletproof as we wanted it to be.

We will strive to explain most of the image processing carried out by inserting nice illustrative images and plots as a complement to the explanatory text. In the very beginning it might be appropriate to explain two systems for representation of colour images, RGB and HSI. Later we will try to visualise the image content using different techniques.

5.1. Image Decomposition

Any description of the human visual system only serves to illustrate how far computer vision has to go before it approaches human ability. In terms of image acquisition, the eye is totally superior to any camera system yet developed. People are continuously trying to improve the existing artificial vision systems. One of the problems to be solved is how to represent colours. Several systems have been invented for this purpose. Here we will only discuss a couple of the most frequently used systems, RGB and HSI.

5.1.1. RGB and HSI spaces. First the RGB system will be presented. RGB stands for red-green-blue. Using these three colours in different amounts almost any other colour can be produced. On a screen mixing is done by having three adjacent dots, one dot for each of the three colours. If these dots are small enough and the observer is far enough away, this gives the appearance of one pixel colour rather than three adjacent ones. These three colours are primary colours, mixing any combination of two of them does not make the third. In fact any three colours could be used, providing they are independent i.e. primary. RGB is the most widely spread colour system.

HSI stands for hue-saturation-intensity. HSI may be regarded as the same space as RGB but represented in a different coordinate system. Hue is effectively a measure of the wavelength of the main colour i.e. there are different numbers representing different colours. E.g. lets say 0 represents red, then move all the way through different colours up to 256, in case we have 256 colours, which again represents red. Imagine a coloured disc that warps around, here 256 is mapped to 0. Saturation is a measure of hue in each spot. If saturation is 0, then the final colour is without hue, i.e. it consists of white light only. Intensity is simply a measure of brightness of each pixel.

Consult Figure 5.1.1 for a visualisation of the colour spaces.

5.1.2. Image Quality. Colour image capture involves the capture of three images simultaneously. With RGB, an early industry standard, intensity of each of red, green and blue has to be measured for each spot. These are then stored in three

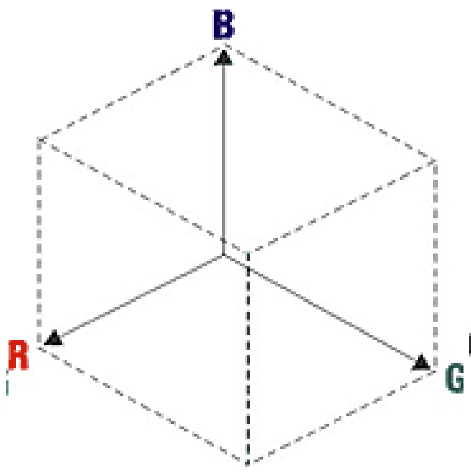

(a) RGB model.

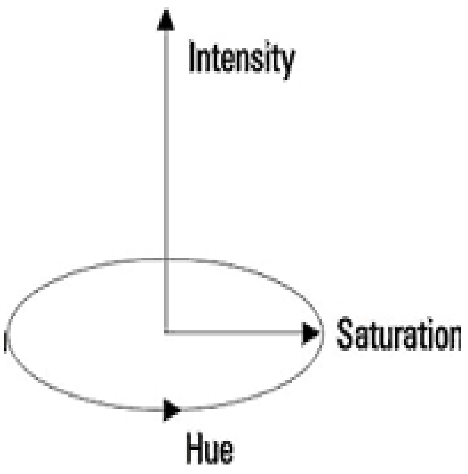

(b) HSI model.

FIGURE 5.1.1. RGB and HSI model representation [7].

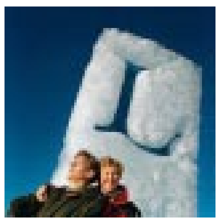
(a) Full color.

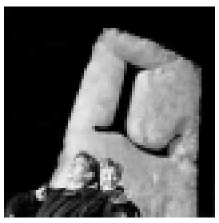
(b) Red component.

(c) Green component.

(d) Blue component.

(e) Grey scale.

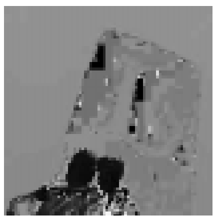
(f) Hue component.

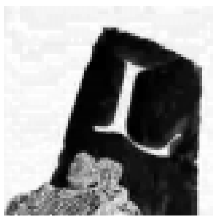
(g) Saturation component.

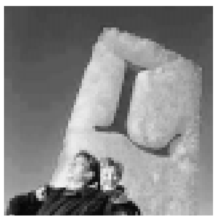
(h) Intensity component.

FIGURE 5.1.2. An image example with its decompositions in RGB, HSI and grey scale.

matrices, every matrix containing the values for one of the colours. In our case every spot in a matrix holds a value representing the intensity of the particular colour. For each spot in every of the three matrices we had eight bits available allowing 256 different values between 0 and 255, where 0 represents the lowest intensity and 255 the highest. Using MATLAB the grabbed images could be transformed into this form. Now further operations could be applied to them in order to retrieve vital information. MATLAB allows also a transition from RGB to HSI and further manipulation of images.

As an example a nice picture taken outside Luleå University of Technology representing the university's logotype engraved in a block of ice, Figure 5.1.2, has been separated into its RGB-components. We can also see the same image in grey scale and its HSI-components. Dissection performed on this image will be used for a quick comparison to our grabbed images.

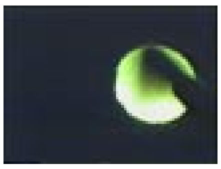
(a) Full color.

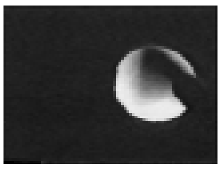
(b) Red component.

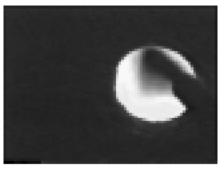
(c) Green component.

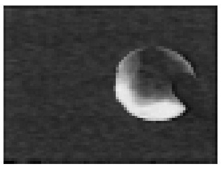
(d) Blue component.

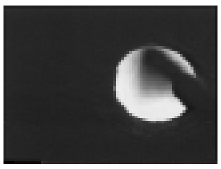
(e) Grey scale.

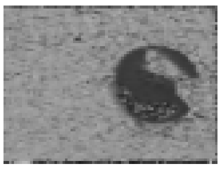
(f) Hue component.

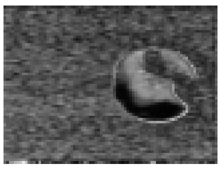
(g) Saturation component.

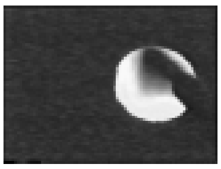
(h) Intensity component.

FIGURE 5.1.3. An image taken with a green glass, with its decompositions in RGB, HSI and grey scale.

Now, decomposing an arbitrary image from inside the blast furnace taken with a green glass in front of the camera gives images in Figure 5.1.3. For RGB, the red and green part look fine whereas the blue one looks different due to the characteristics of the filter. For HSI, the hue and saturation buffers are very noisy and therefore hard to deal with. The intensity component is quite alright though. Hue and saturation can be compared to the ones in Figure 5.1.2 where no noise is present.

Finally the same was done to an arbitrary chosen image from the film sequence filmed with a transparent glass, Figure 5.1.4. Blue component of the RGB looks better here than in the previous series. It would therefore be advantageous to use transparent glass. Evidently, being able to use three channels instead of two would increase the redundancy when approximating the pulverised coal flow. A restriction here are the cameras used. The very bright light makes even the better cameras saturate. That is clear in the saturation component in Figure 5.1.3, the lower area of the interior of the blast furnace, and in Figure 5.1.4 it is visible on the edges around the peek hole. Fortunately, strictly measuring the flow should not be affected too much by cameras saturating for pixels surrounding the plume. Temperature measurements of the flame would be much more problematic. Looking into the hue, saturation and intensity buffers we can conclude that there is still noise present for hue and saturation although it looks sharper than previously. The intensity component is not remarkably affected, it look more alike the grey scale image than it did in the image taken with green glass.

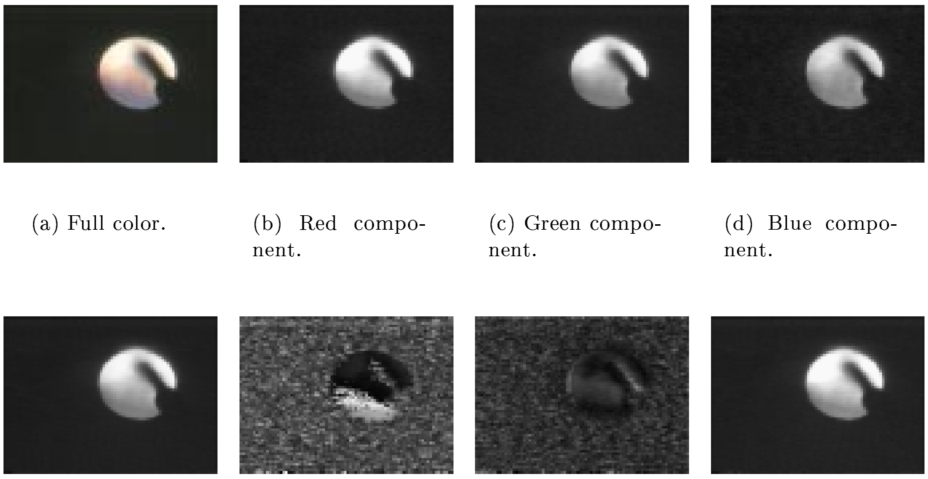

(a) Full color. (b) Red component. (c) Green component. (d) Blue component.

(e) Grey scale. (f) Hue component. (g) Saturation component. (h) Intensity component.

Figure 5.1.4. An image taken with a transparent glass, with its decompositions in RGB, HSI and grey scale.

5.2. Image Content

An important issue is to find the difference between a coal free image and another one with coal. A coal free image does not mean a gas free image, nor does it mean an activity free image. It is only an image that seems to have less coal than other images in general. This differences might be viewable when looking at the intensity histograms of the picture. Another issue is figuring out where to look for the plume, the flame and the gases.

5.2.1. Image Histograms. n Figures 5.2.1 and 5.2.2 we see images with their corresponding histograms. First we have RGB decomposition of the pictures and then HSI components. The upper part of each figure is taken with a green glass and the lower part is taken with a transparent glass, the left side represents coal free images and the right side represents images with coal.

In the RGB domain, Figure 5.2.1, searching the histograms of the images we can make some observations. Starting with the green glass images and their RGB decomposition, the green component is saturated in both images. From the red components we can conclude that gases have an intensity value just below 50 in those images. The blue component of the coal free image has other characteristics than the other components, but the red and green components are slightly similar. If we assume that the green glass is not harmful to the image contents, then we have an unanswered question. What do we see there? We will try to answer this question later in Chapter 5.2.2. We notice a slight shift from the high intensities to the low ones when we move from a coal free image to one with coal. This is because obviously the first hill represents mostly the coal in the picture. The conclusion is that we can, by comparing histograms, determine if there is coal present or not. This phenomenon is even seen in the blue component which is the most noisy one.

Comparing the images taken with the transparent glass and the green glass we notice that the width of the first hill in the histograms changes. The first hill in the histogram located at around value 50 is much wider when coal is present. Interesting

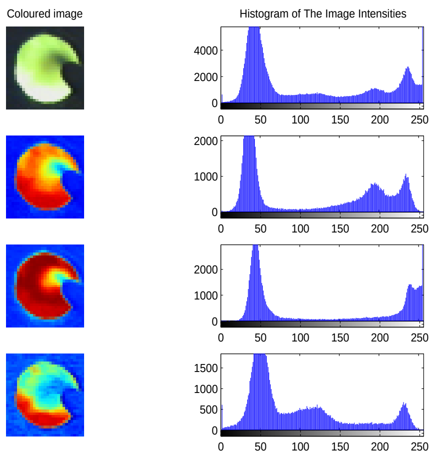

(a) Based on an image taken with a green glass, without coal.

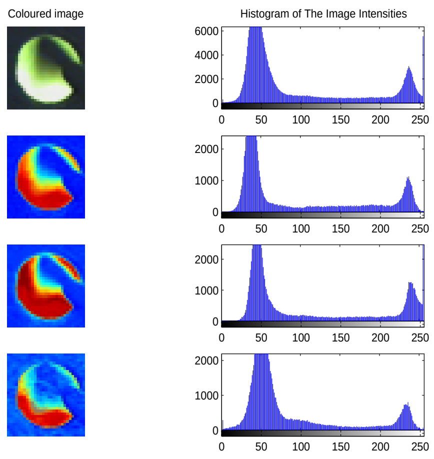

(b) Based on an image taken with a green glass, with coal.

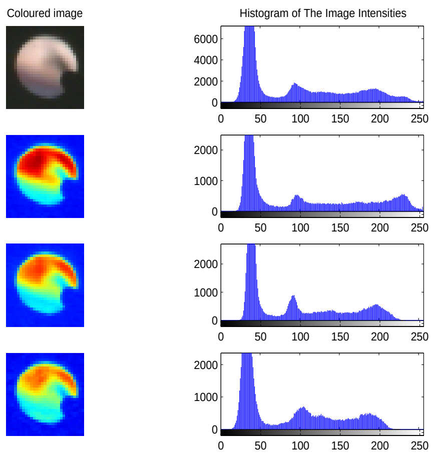

(c) Based on an image taken with a transparent glass, without coal.

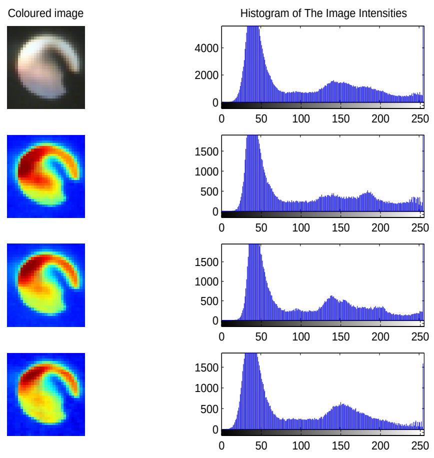

(d) Based on an image taken with a transparent glass, with coal.

FIGURE 5.2.1. A comparison of image intensities in the RGB-space.

enough the green and blue histograms for the coal free image do not reach above 220, those buffers are not saturated. In fact the red component is not saturated either. This is not the case in the image with coal except for the blue component. Those shifts in the colour scale are quite interesting in temperature analysis and are not found in the images taken with green glass. Notice also that in those images we do have something in the intermediate register between the brightest and the darkest hills. This was not present in the pictures taken with the green glass. It might be an effect of better camera dynamics. The only difference here is that green glass images contain more noise, especially for the blue component.

Moving over to the HSI domain it is easy to see that the hue and saturation parts are noisy, possibly due to overexposure. Use of different types of glass does not affect the level of noise considerably. The intensity part is however not disturbed.

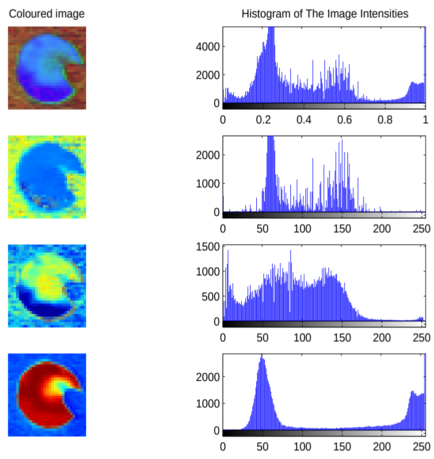

(a) Based on an image taken with a green glass, without coal.

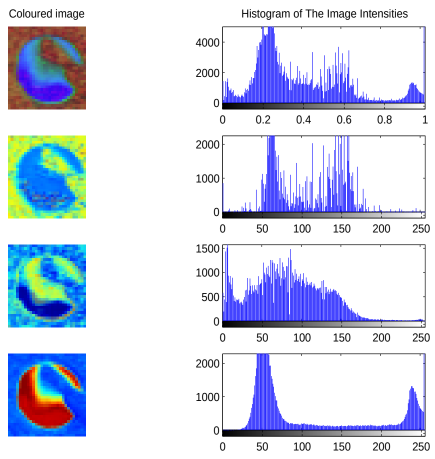

(b) Based on an image taken with a green glass, with coal.

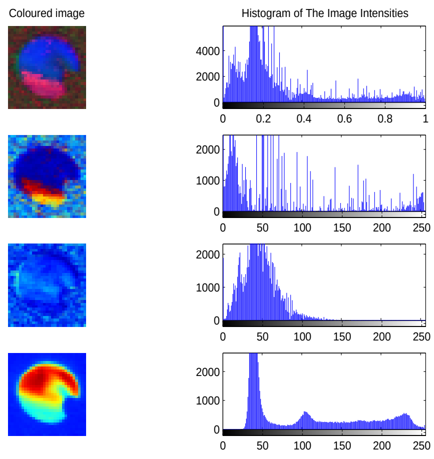

(c) Based on an image taken with a transparent glass, without coal.

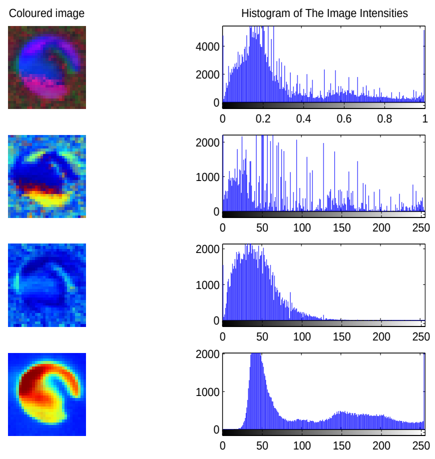

(d) Based on an image taken with a transparent glass, with coal.

FIGURE 5.2.2. A comparison of image intensities in the HSI-space.

It is easily seen that the first hill in the histogram for the intensities reflects the amount of pulverised coal present. We see a clear colour shift when changing the glass. The histograms of the hue and saturation are not fully occupied, a possible opportunity for histogram stretching appears. We can see which values are the most frequent ones when coal appears in an image, but the problem is that those values are not only reserved for the coal. Other elements in the image share the same space.

Looking at the height and the width is the first approach. Also we could think of comparing the low intensity part of the histogram to the high intensity part. This could be done by forming a ratio between those after dividing the histogram in half. A high ratio value would indicate coal whereas a low one would mean that a minor amount of coal is present. It has to be pointed out that again we do not know which part is coal and which are just gases formed inside the blast furnace, since both seem to be present in the same place in the histograms.

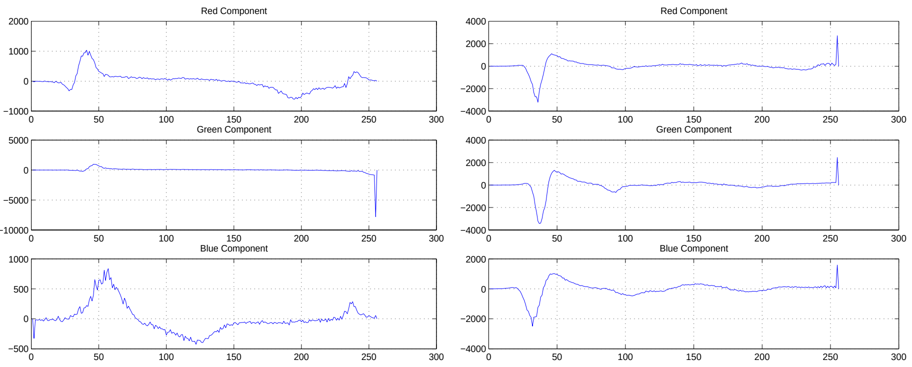

(a) Difference of images taken with a green glass.

(b) Difference of images taken with a transparent glass.

FIGURE 5.2.3. Difference in the histograms in RGB-space. The x-axes represent intensities and the y-axes are the difference in pixels.

It might be hard to draw all the conclusions from the former figures. Another way of seeing the same thing is subtracting histograms of the coal free images from those with coal. The result is illustrated in Figure 5.2.3 and 5.2.4. The positive values represent intensities found in the images with coal and the negative values are those found in images without coal.

In the RGB-space we see that the blue component of the images taken with a green glass is quite noisy. Also the red one is a little bit so. The three buffers in 5.2.3-(a) are different, no specific characteristic, on the other side 5.2.3-(b) are more or less three identical graphs.

Inspecting the HSI-space, the two histogram sets show different behaviour. The noise in the hue and saturation components is clear. Concentrating on the histograms of the images taken with the green glass we can see in an image with no coal values, 50-65, that are missing in an image with coal for the hue component. The same phenomenon is visible between 115-175 for the saturation component and above 250 for the intensity component. This is not true for the images taken with the transparent glass. A clear impact of changing the glass can be seen, which effects can not be addressed to the change of camera. The intensity component graph is almost a copy of the RGB-components graphs for the same images, that is usually the case in a healthy image.

We can see where we can expect coal and where we do not. A way to emphasise the difference between the coal and no coal in the images is to multiply each image histogram by the difference histogram we saw in the figures above, before any further image processing, in order to find the plume.

5.2.2. Image Threshold. To see if there is any definite threshold that can separate the background from the interesting elements, the coal from gases and so forth, we took the pictures we used above, decomposed them into their RGB-components, quantised them linearly with ten steps and thresholded at those steps. The steps used were between 0 and 1 with a step size of 0,1. Studying Figure 5.2.5 and 5.2.6 shows that threshold values can be examined in more detail. Evidently

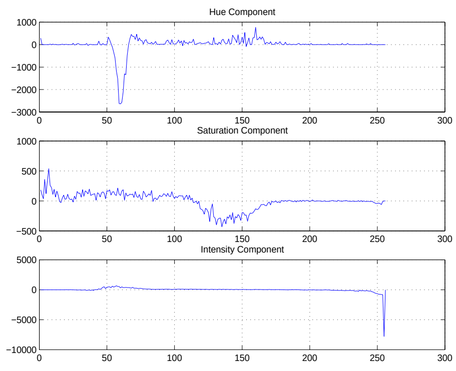

(a) Difference of images taken with a green glass.

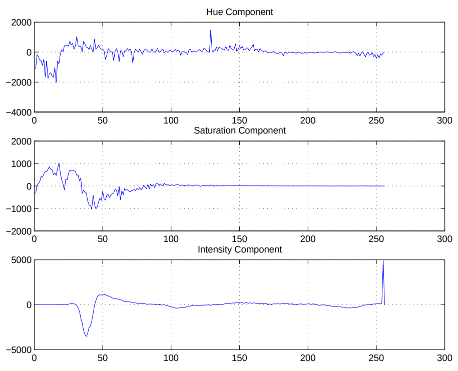

(b) Difference of images taken with a transparent glass.

FIGURE 5.2.4. Difference in the histograms in HSI-space. The x-axes represent intensities and the y-axes are the difference in pixels.

the plume's size and to some extent also the shape changes are dependent on the chosen threshold value. This is seen when looking at what parts of the image belong to which shade for the three colour buffers.

Figure 5.2.5 is based on images taken with a green glass. In general, the images show that the coal including the background is found between 0,1 and 0,5. The background should be separated from the coal somewhere in between 0,1 and 0,2 and the gases lie between 0,5 and 0,9. The foreground is seen at the lower part of the images. The blue components are kind of special, the last two thresholds are reserved for the foreground. That could be something related to the temperature of the foreground. The plume has a different shape here and is getting bigger. There are clearly elements that have a breakthrough in the blue component. Maybe the green glass has enhanced it even more.

Next stop is on Figure 5.2.6 where we have images taken with a transparent glass. The first thing to notice is that the plume is smaller. Overexposure? We believe that the plume is distorted. Different thresholds do not give separate areas in general. It is easier here to see the background. There is almost no coal at 0,2.

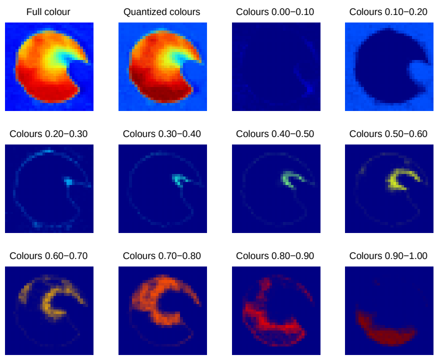

(a) Red component, image without coal.

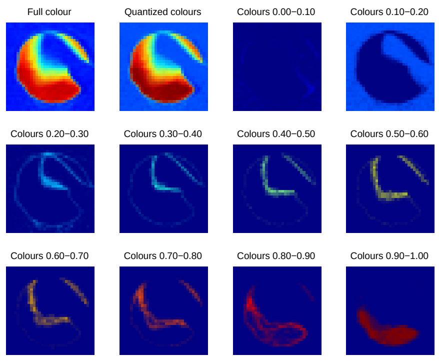

(b) Red component, image with coal.

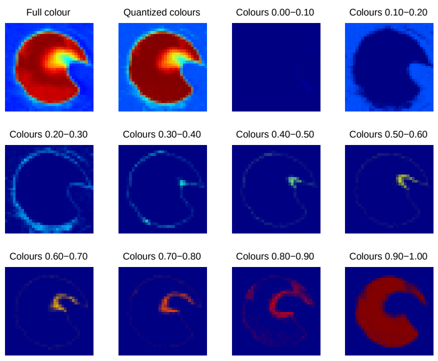

(c) Green component, image without coal.

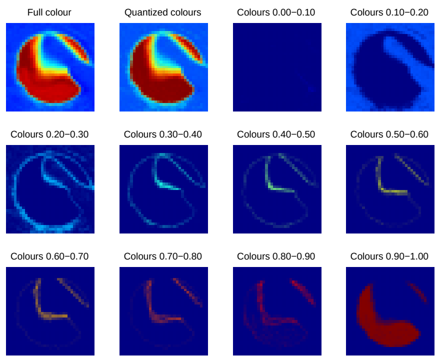

(d) Green component, image with coal.

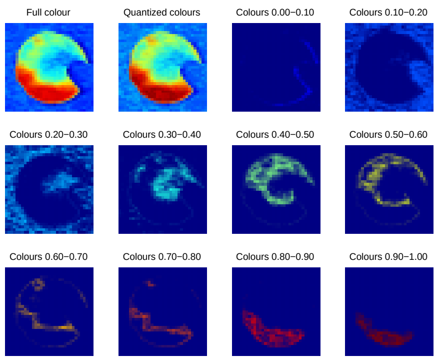

(e) Blue component, image without coal.

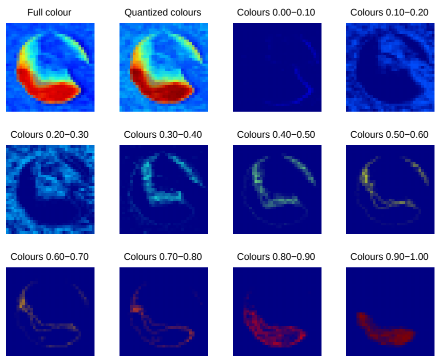

(f) Blue component, image with coal.

FIGURE 5.2.5. RGB components, based on images taken with a green glass. Thresholded between 0 and 1 with steps of 0,1.

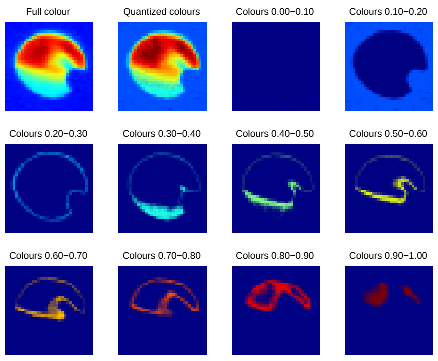

(a) Red component, image without coal.

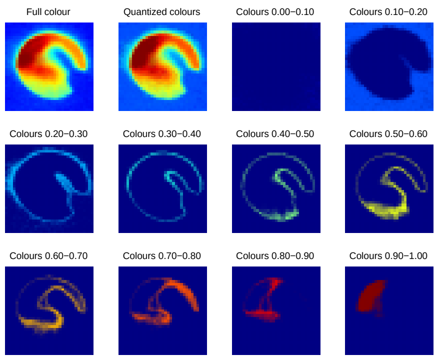

(b) Red component, image with coal.

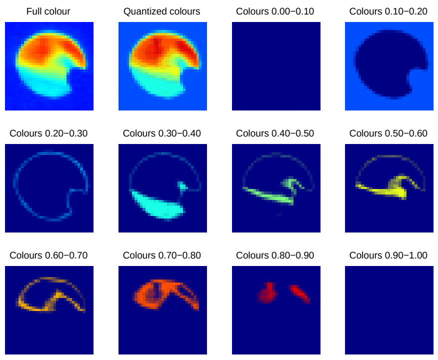

(c) Green component, image without coal.

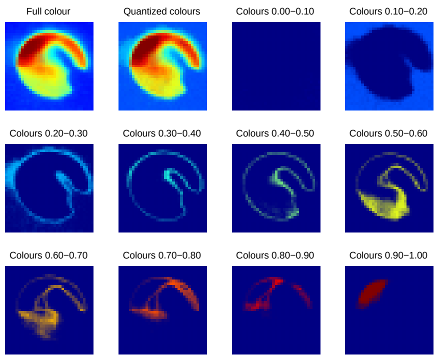

(d) Green component, image with coal.

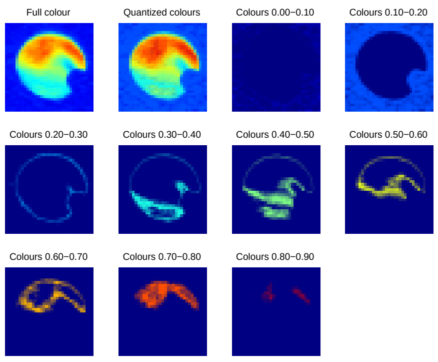

(e) Blue component, image without coal.

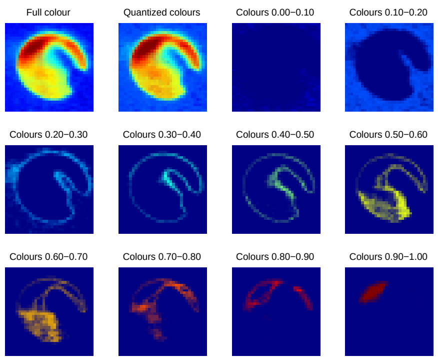

(f) Blue component, image with coal.

FIGURE 5.2.6. RGB components, based on images taken with a transparent glass. Thresholded between 0 and 1 with steps of 0,1.

CHAPTER 6

Algorithms

Here procedures for extracting information from video sequences will be discussed as well as a few useful algorithms designed to calculate changes in the pulverised coal flow. Beginning with finding a static background used to mask out the coal plume, we will move through an alternative method of finding a background for every image, finding the coal plume and last we will introduce three algorithms for continuously approximating the volume of coal material injected i.e. a possible replacement measurement for the currently used flow measurement. We will also try to point out possible drawbacks of the algorithms.

Starting with an image of coal injected into a blast furnace we need to end up with data that can be used in our steel making process. We need to calculate coal flow, flame temperature and coal distribution data. While we are not handling the temperature and coal spreading parts in this report we will concentrate on the coal flow, emphasising that the same ideas apply for all three parts. Remember that we have colour images, that means we have several information channels that can be combined after processing them separately. The algorithms listed below handle a single information channel of the image if nothing else is mentioned explicitly. All the discussed algorithms are implemented, see Appendix , and tested in MATLAB. See Chapter 7 for further investigation of the implemented algorithms used with our data.

The steps from an image to a fully useful flow data can be outlined as follows:

- Finding the image background.
- Finding the coal plume.
- Finding the plume's volume.
- Conversion between volume and flow measurement.

The first three points are dealt with next.

6.1. Finding the Background

A background is the dark area in the image representing the protecting pipe and the visible part of the tuyere. Finding a suitable background is a first step in isolating the plume in every sampled image. The need of a background will be explained in Chapter 6.2. The following discussion covers two different investigated approaches for finding the background mask, a black and white image (binary image). We want to keep apart the use of two terms throughout this report: plume and flame. By plume we mean the coal particle cloud being injected through a tuyere meanwhile flame refers to the surrounding burning area which might include gases.

6.1.1. One Background Approach.

The first background approach is to search for an image with a small amount of coal powder visible. Reasonably one would argue that the best way of finding the plume would be to find the right threshold values, first finding the background and then extracting the plume. The shortcoming of this method is obvious in our case. In our images the plume, the visible part of the tuyere and everything around the opening in the blast furnace wall is very dark. Under those conditions there is no simple way of distinguishing the coal plume from other parts. The same problem is encountered in both RGB buffers as well as HSI buffers.

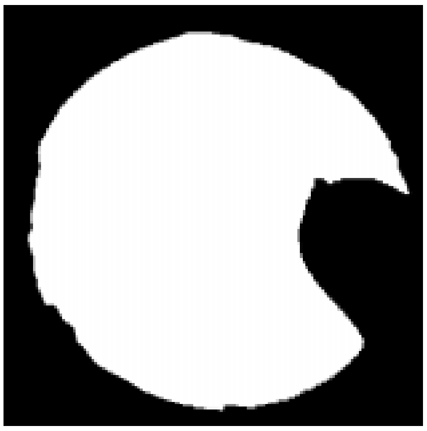

FIGURE 6.1.1. A typical fixed background image.

Establishing that thresholding is not sufficient means of recovering the background from our images, we have to think of slightly more advanced solutions. One possibility is to look for an image containing very small quantities of coal and then thresholding to obtain a nice background without any trash. As long as we can find an image not containing too much coal this works. The drawbacks are that it might be hard to find an appropriate image and that the cameras are not fixed, which means that if someone would accidently bump into one of them, the whole image would move and suddenly our background would not fit the picture i.e. a new background mask would have to be found. The same applies to zooming, where the operators usually have the possibility to do. Of course there is a simple cure to this problem, fixing the cameras while the blast furnace is in use, and banning the operators from doing any adjustment. Alternatively one can have a procedure of taking fresh new coal free images every time the camera setup is changed. A useful background image mask that can be used to remove all the uninteresting details is in Figure 6.1.1.

6.1.2. Customised Background Approach. The one background approach is sufficient in most the cases, but it has several limitations. If a worker happened to touch the camera housing causing some trembling, then the extracted data sequence should be trashed until the camera settles. An operator can control the camera position, focus and zoom. Any of these actions and any calculations based on one fixed background is faulty. Most importantly, we want a system that is as easy as possible and can automate most of the work with minimum interaction from the operators. No one in the industry has time to grab a coal free image every time something changes in the camera setup or its surrounding environment. A need of finding the background in every image is unavoidable.

Knowing that the colour of the coal is the same as, or at least very close to, the colour of the tuyere and the surrounding area makes finding the background a hard task. Several algorithms have been looked at in order to evaluate which one gives most satisfactory performance.

The easiest thing to do is just thresholding the images and doing some morphological operations to clean up unwanted trash and fix the shape of the background.

Algorithm 1 Imfilter

```
imfilter($im$, $y$)
1.  $pim \leftarrow$ zero pad $im$ with $2{\cdot}y$ pixels, around $im$
2.  $mask \leftarrow y \times y$ zero matrix surrounded by ones
3.  $irows \leftarrow$ **rows**($im$)
4.  $icols \leftarrow$ **columns**($im$)
5.  **for** $r \leftarrow y+1$ **to** $irows+y$
6.      **for** $c \leftarrow y+1$ **to** $icols+y$
7.          **if** $pim[r, c]$ **then**
8.              $tmp \leftarrow pim[r\text{-}y..r+y,\ c\text{-}y..c+y] \odot mask$
9.          **if** **sum**($tmp$) $= 0$ **then**
10.             $pim[r\text{-}y..r+y,\ c\text{-}y..c+y] = 0$
11.         **end**
12.     **end**
13.   **end**
14. **end**
```

Typical cleaning up operations are: erosion, dilation, shrinking and filling. The problem with this simple algorithm outline is that we believe, from our examination of the images in Chapter 5, that there is no such a threshold that could guarantee us a good background image. Compromises have to be made and more advanced algorithms have to be implemented in order to eliminate the bad effects of the compromises. Filtering can be used to remove any unwanted small objects that are not possible to eliminate with the previously mentioned operations. Algorithm 1 does such kind of filtering, it looks for islands, isolated pixels, and removes them according to the filter parameter which decides the size of the unwanted objects.

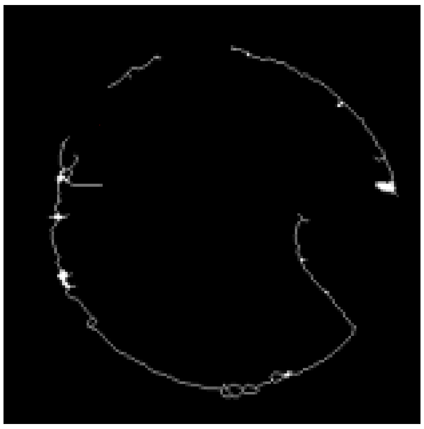

FIGURE 6.1.2. Edge detection containing some discontinuities.

Different threshold values can be used to find the edges in an image. In our case the most prominent edges are those between the peek hole's edges with the tuyere and the inside of the furnace but also the coal particle cloud and the furnace interior. If we could find a reasonable threshold that gives us the first mentioned edges then we are done. This is the same problem as the one we mentioned in the simple algorithm we started with above. Tests have shown that it is possible, most of the time, to choose a threshold that can be used to edge detect the image and keep parts of the most interesting edges. The result of such edge detection looks like the one in Figure 6.1.2. What we need to do in order to recreate our background is retie our disconnected edge parts.

Algorithm 2 Imends

```
                         imends($im$)
 1. $mask \leftarrow \begin{bmatrix} 07 & 11 & 13 \\ 17 & 00 & 19 \\ 23 & 29 & 31 \end{bmatrix}$
 2. $order \leftarrow \begin{bmatrix} 01 & 02 & 03 \\ 04 & 00 & 05 \\ 06 & 07 & 08 \end{bmatrix}$
 3. $eim \leftarrow 0$
 4. $irows \leftarrow$ **rows**($im$)
 5. $icols \leftarrow$ **columns**($im$)
 6. **for** $r \leftarrow 1$ **to** $irows$
 7.    **for** $c \leftarrow 1$ **to** $icols$
 8.      **if** $im[r, c]$ **then**
 9.        $tmp \leftarrow$ the nine pixels surrounding $im[r, c]$
10.        $isum \leftarrow$ **sum** ($mask \odot tmp$)
11.        **if** $isum \in mask$ **then**
12.          $dir \leftarrow$ get the $order$ of $isum$ in $mask$
13.          $eim[r,c] \leftarrow dir$
14.        **end**
15.      **end**
16.    **end**
17. **end**
```

Connecting edge parts like these is an easy task for a human equipped with a pencil, but it is harder for a computer to accomplish the same thing. Algorithms exist to connect parts/pixels representing a regular shaped pattern. What we have here is a circle with a part of a tuyere inside; this is a tough one. Closer examination has shown that we can assume that each two adjacent edge section's endpoints facing each other should be connected to create a continuous edge. We can also look at the direction of each edge part's endpoints before we connect it to anther endpoint. In this manner we try to trace through the edge parts in order to connect them all. Finding those endpoints, the edge part they belong to and the direction they are pointing in is done using Algorithm 2. This algorithm takes a binary image with disconnected edges and returns the possible endpoints and their direction encoded as a digit 0-8, where 0 is no connection and is imply an isolated pixel. In this algorithm we look at the eight-neighbouring pixels for each pixel before deciding anything. A pixel is regarded as an endpoint if it is only connected to one of its neighbours. We have to ensure ourselves that the edges are one pixel wide, otherwise we need to look at more than the eight-neighbouring pixels to determine whether a pixel is an endpoint or not.

A problem we still need to deal with are all the T-connections, as shown in Figure 6.1.3; those endpoints that are not to be connected are called ghost endpoints. As you can see there is no doubt about how the green points should be connected ($8 \to 7$ and $6 \to 5$). It is not obvious knowing which point should be connected to 4. The right answer is 3 and in this case 1 and 2 are the ghost endpoints. They should either be removed from the endpoint list returned by Algorithm 2 or dealt with later in an algorithm that uses it.

Having the endpoints selected, it is time to move on and connect them. This is accomplished with Algorithm 3, based on the ideas presented earlier in this section.

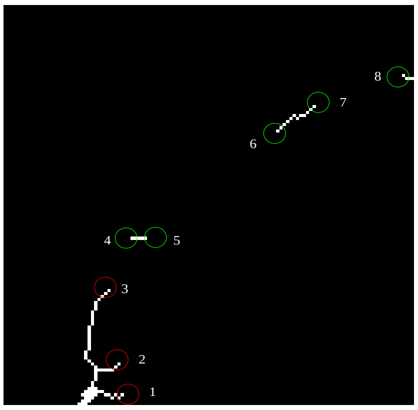

FIGURE 6.1.3. T-connections and ghost endpoints.

Algorithm 3 Imconnect

```
imconnect($im$)
1. $oim$ ← find and identify the objects in $im$
2. $eim$ ← find the pixels representing the endpoints of the objects in $oim$
3. $dis$ ← calculate the distances between all the pixels in $eim$
4. $cim$ ← $im$
5. while there are unconnected objects in $oim$
6.     $p1$, $p2$ ← find the pixels with shortest distance in $dis$ between non-connected objects according to $oim$
7.     $cim$ ← $cim$ + connect $p1$ and $p2$
8.     update $oim$ by making the objects that $p1$ and $p2$ belongs to one object
9. end
```

Thus connecting the edges with a reasonable result is possible. This algorithm starts with an image that has disconnected edge parts, identifies them, finds the endpoints and makes a list of the object they belong to, calculates the distance for all possible connections between the endpoints (watching out for ghost endpoints), looks for the minimum distance, makes a connection between the two parts and updates the endpoint list to regard the last connected parts as one part. The algorithm does this until we have only one object in our image with no disconnections. An auxiliary algorithm, Algorithm 4, is used to draw a line between two endpoints in an image given their coordinates.

Back to our initial subject, finding the background. Algorithm 5 lists the needed steps. Edge detecting, morphological filtering, connecting any disconnected edges and finally filling the resulting object with ones to get the black and white background.

In a short run the background image is static, the happenings are restricted to the inner parts of the furnace. If we stack several succeeding images, the static part of the images will be dominating. The background can now be regarded as the most significant pixels, those that are repeatedly found in most of the images within the stacked bunch. It is now easy to find the edges surrounding the interesting area. Algorithm 6 shows how this is done.

Similar approach is made in Algorithm 7, apart from the fact that we stack the edges found in the images instead of the images themselves. Decisions have to be

Algorithm 4 line2pixels

```
line2pixels($x1$, $y1$, $x2$, $y2$)
1. $m \leftarrow \frac{y2-y1}{x2-x1}$
2. $b \leftarrow y2$ - $m \cdot x2$
3. $r \leftarrow []$
4. $c \leftarrow []$
5. if $y1 < y2$
6.   $r \leftarrow y1$ .. $y2$
7. elseif $y2 > y1$
8.   $r \leftarrow y2$ .. $y1$
9. end
10. if $x1 < x2$
11.   $c \leftarrow x1$ .. $x2$
12. elseif $x2 > x1$
13.   $c \leftarrow x2$ .. $x1$
14. end
15. if $c$ = nil
16.   $c[1..$length$(r)] \leftarrow x1$
17. elseif $r$ = nil
18.   $r[1..$length$(c)] \leftarrow y1$
19. else
20. $ci \leftarrow$ round$\left(\frac{r-b}{m}\right)$
21. $ri \leftarrow$ round $\left(\frac{m \cdot c}{b}\right)$
22. $cpix \leftarrow$ append$(c, ci)$
23. $rpix \leftarrow$ append$(r, ri)$
```

Algorithm 5 Imback

```
imback($im$, $th$)
1. $eim \leftarrow$ edge detect $im$ according to $th$
2. $mim \leftarrow$ clean up $eim$ using morphological operations
3. $cim \leftarrow$ connect the objects $mim$
4. $bg \leftarrow$ fill $cim$'s inside with 1:s
```

Algorithm 6 Bgmulti

```
bgmulti($ims$, $layers$)
1. $ok \leftarrow 0$
2. $tmp \leftarrow 0$
3. for $i \leftarrow 1$ to (length$(ims)$-$layers+1$)
4. while $ok < layers$
5.       $tmp \leftarrow ims[1..end, 1..end, ok+i] + tmp$
6.       $ok \leftarrow ok + 1$
7.   end
8.   $mtmp \leftarrow \frac{tmp}{layers}$
9.   $eim \leftarrow$ edge detect $mtmp$
10.   $eims[1..end, 1..end, i] \leftarrow$ clean up $eim$ using morphological operations
11.   $ok \leftarrow ok$ -1
12.  $tmp \leftarrow tmp$ - $ims[1..end, 1..end, i]$
13. end
```

made about how many images to stack and when a pixel is counted as static or not. Final polishing is done with some well chosen morphological operation sequence.

Algorithm 7 Bgmultiedge

```
bgmultiedge($ims$, $layers$, $accept$)
 1. $ok \leftarrow 0$
 2. for $i \leftarrow 1$ to (length($ims$)-$layers$+1)
 3.    while $ok < layers$
 4.       $eims[1..end, 1..end, ok+1]$ ← edge detect $ims[1..end, 1..end, ok+i]$
 5.        $ok \leftarrow ok + 1$
 6.    end
 7.    $tmp$ ← sum $eims$ layers pixel wise
 8.    $bg \leftarrow tmp \geq accept$
 9.    $bgs[1..end, 1..end, i]$ ← clean up $bg$ using morphological operations
10.    $ok \leftarrow ok - 1$
11.   $eims$ ← shift_left($eims$)
12. end
```

In a well controlled plant there always exists a certain coal flow, which makes this algorithm fail in finding the real background. It simply assumes the areas close to the tuyere's mouth to be part of the background, when they do not change, and the sharp edge between the tuyere and the coal is gone. The result is a discontinuous edge. This effect is illustrated in Figure 6.1.4. The best thing we can do is connecting the discontinuous parts using the algorithm we discussed earlier, but the tuyere shape is still not perfect.

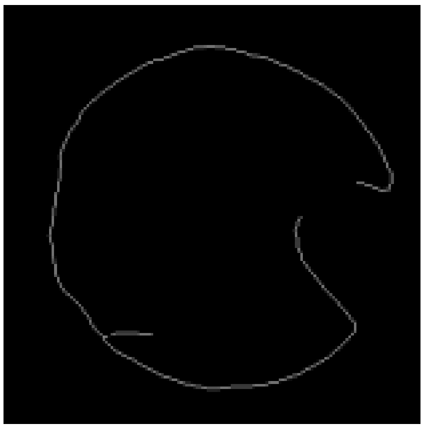

FIGURE 6.1.4. Multiple layer edge detection.

The bigger an image is the more CPU and time is needed to process it. Because the nature of our images, a hot spot surrounded by a static dark part, we need only to process the interesting part of them. The area of interest is not always in the same location in a flexible system, that is why we need to find the area in every single frame we want to process. This is done with Algorithm 8. This algorithm basically scans the image for light pixels. The rectangular area with a lot of light pixels inside is the most interesting part of the image. Combining this with the previously mentioned background algorithms will make them faster.

Algorithm 8 Dyncrop

```
dyncrop(*im*)
1. $csum \leftarrow$ sum of the pixels in $im$ column-wise
2. $rsum \leftarrow$ sum of the pixels in $im$ row-wise
3. $cth \leftarrow$ calculate a column threshold
4. $rth \leftarrow$ calculate a row threshold
5. $cint \leftarrow csum > cth$
6. $rint \leftarrow rsum > rth$
7. $cim \leftarrow im[rint, cint]$
```

Algorithm 9 is a modified version of Algorithm 5. It does pretty much the same thing beside it starts with median filtering of the image and finds the interesting area in it before further processing.

Algorithm 9 Dynbg

```
dynbg(*im, th*)
1. $fim \leftarrow$ median filter $im$
2. $ifim \leftarrow$ find the interesting area in $fim$
3. find $th$ for $ifim$ if $th$ is not given
4. $e \leftarrow$ edge detect $ifim$ according to $th$
5. $em \leftarrow$ enhance $e$ using morphological operations
6. $cim \leftarrow$ connect the edges in $em$ if needed
7. $bg \leftarrow$ fill $cim$'s inside with 1:s
```

To summarise: The best approach in order to find the background is stacking several consecutive images, crop the resulting image, edge detect it, improve the edges by morphological operations, connect any discontinuous edges and finally fill the inside with ones. The result typically, although exceptions exist, looks like the one in Figure 6.1.5, which can be compared to Figure 6.1.1.

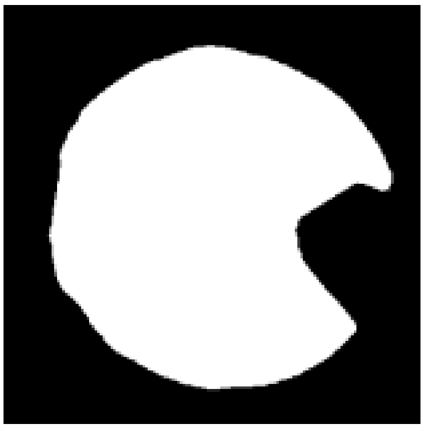

FIGURE 6.1.5. A background using the suggested algorithm approach.

6.2. Finding the Coal Plume

Having nice background we can effortlessly find the coal plume. What we basically have to do is just to subtract each image from its background and then

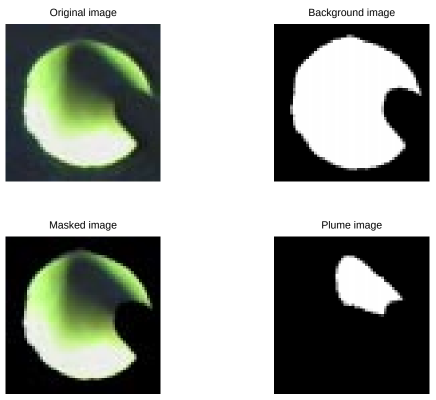

(a) Based on an image taken with green glass.

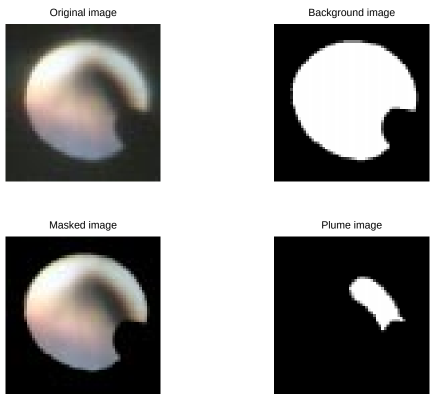

(b) Based on an image taken with transparent glass.

FIGURE 6.2.1. Plume extraction.

threshold it. In result we obtain the coal plume. This operation is illustrated in Figure 6.2.1. There is some decision making problem here: What should we regard as the coal plume? We know for sure that there is no sharp edge between coal and the gases inside the furnace. Also it is not obvious what threshold value should be chosen. Depending on the threshold value chosen, the coal cloud has different sizes and sometimes even slightly different shapes, although it is always close to being elliptic. Choosing the correct threshold involves distinguishing between coal and gases in the image, which is not completely unequivocal. Figure 6.2.2 shows the same plume extracted with different thresholds. Notice well, plumes with high thresholds are not of any use in the video series taken with transparent glass but are quite nice in the green glass case.

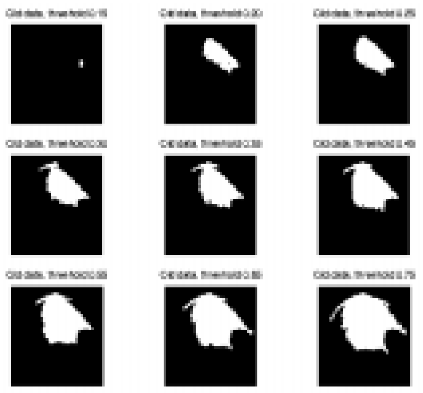

(a) Based on an image taken with a green glass.

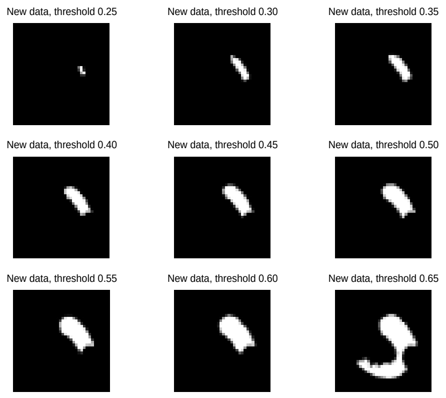

(b) Based on an image with a transparent glass.

FIGURE 6.2.2. Size of the plume depending on threshold value.

Algorithm 10 Findplume

```
findplume($im$, $bg$, $bwth$, $th$)
1. $bwim \leftarrow im > bwth$
2. $csum \leftarrow$ sum of the pixels in $bwim$ column-wise
3. $rsum \leftarrow$ sum of the pixels in $bwim$ row-wise
4. $cint \leftarrow csum > th$
5. $rint \leftarrow rsum > th$
6. $roi \leftarrow bwim[rint, cint]$
7. $fim \leftarrow (1\text{-}roi) \odot bg$
```

We have been looking at two algorithms in order to obtain a good result. Algorithm 10 is used when we do not know where the background mask fits in the image. First we threshold the given image, find where the background best fits and then we remove the unwanted objects by multiplying the thresholded image with the background and voilà the plume is there. The second algorithm, Algorithm 11, is for the case when we know where to place the background on the image. Also here we start with thresholding the image, use morphological operations to get rid of unwanted objects and finish with morphological filtering, Algorithm 12, in case the earlier morphological operations were not enough. This filtering can also be executed as the last stage of Algorithm 10.

Algorithm 11 Implume

```
implume($im$, $th$, $bg$, $x$, $y$)
1. $nim \leftarrow bg$ - $(im > th)$
2. $mim \leftarrow$ clean up $nim$ using morphological operations
3. $fim \leftarrow$ identify the flame in $mim$ knowing its originate from $(x, y)$
```

Algorithm 12 Plumeident

```
plumeident($im$, $th$, $x$, $y$)
1. $lim \leftarrow$ identify the objects in $im$
2. for $i \leftarrow 1$ to the number of objects in $lim$
3.     $isum \leftarrow \textbf{sum}(lim[i])$
4.     if $isum > th$
5.         $xc, yc \leftarrow$ find the centre of $lim[i]$
6.         $dist[i] \leftarrow \sqrt{(y-yc)^2+(x-xc)^2}$
7.     else
8.         $dist[i] \leftarrow 0$
9.     end
10. end
11. $mindist \leftarrow \textbf{min}(dist) \neq 0$
12. $fim \leftarrow lim[mindist]$
```

The need of morphological filtering arose when we started to process the video signal from our third signal collecting session, where the images tend to be overexposed and thresholding gave sometimes several unwanted objects beside the plume itself. You can see the difference for yourself in Figure 6.2.3.

The idea behind the algorithm is first identifying the different objects in the image, followed by removing the smallest of them according to a given value. Then by knowing the tuyere's position in the image, the distance between that point and

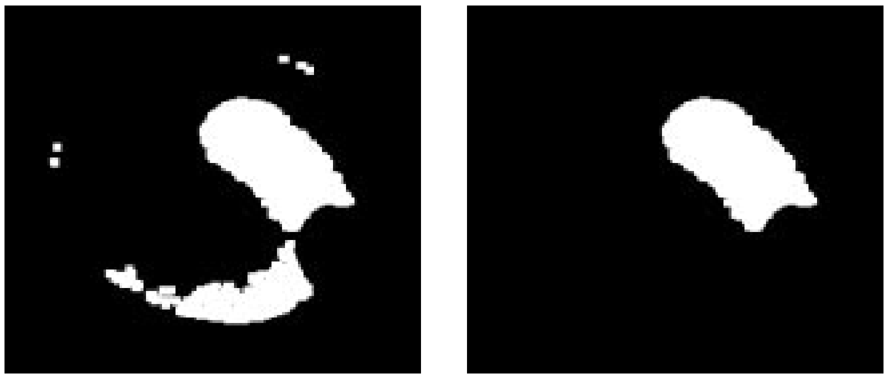
(a) Before using the algorithm. (b) After using the algorithm.

FIGURE 6.2.3. Morphological filtering, using Algorithm 12.

centre of every object left can be calculated to finally choose the object with the shortest distance.

6.3. Estimation of Plume's Area

Having isolated the plume from the rest of the image we could easily calculate its size in pixels. The number of white pixels in the picture is determined and the resulting value describes the size of the coal particle cloud and its density. We have to be aware of that flow is given by the volume of the particle cloud. As an a priori study we can use the area of the plume to represent pulverised coal flow.

6.4. Estimation of Plume's Volume

The area of a two-dimensional plume in the film sequence is easily calculated, however the three-dimensional pulverised coal body is what we are looking for. Estimating the volume of the coal cloud is not an easy task. First of all we see the cloud from an angle. Secondly we do not know what form this cloud possesses in three dimensions, having only access to its two-dimensional projection. We have to make an assumption about its shape. Three different approaches to estimate the volume of the pulverised coal cloud will therefore be discussed here. None of these gives us the actual flow. Using these algorithms we will obtain numbers representing the flow, which can be compared to numbers in the same series i.e. we can conclude if the flow is increasing, decreasing or staying at the same level. However, small future adjustments should allow using these values for real measurement, where the flow is given in grammes per second. What still has to be done is deciding what value corresponds to what flow, which should be a part of a further study. Being able to translate evaluated values to grammes per second, we will have a good measurement of the flow just using image processing.

6.4.1. Weighted Pixel Estimation. The first more advanced attempt to make an approximation of the volume of the pulverised coal cloud seen in the grabbed images discussed in this report will be the Weighted Pixel Estimation. Weighted Pixel Estimation is based on the fact that the cloud is not uniformly dark. This implies that in the middle of the cloud there is more coal than on the edges where it is not at all as dark. We can establish that the size of the cloud is dependent on the chosen value for thresholding of the image. Giving all the pixels belonging to the thresholded plume the same importance is clearly unfair. Common sense suggests weighting pixels so that darker pixels are weighted heavier. Although this seems to be a reasonable solution there are no definite rules for this kind of weighting. In our case it came to be, more or less, all about trial and error for how the weighting should be arranged. More knowledge about the spreading of coal injected into the blast furnace and metallurgical competence would probably help when deciding the weighting.

Algorithm 13 Imweight

```
                    imweight($im$)
1. $imax \leftarrow \mathbf{max}(im)$
2. $imin \leftarrow \mathbf{min}(im) \neq 0$
3. $nim \leftarrow imax\text{-}im\text{+ } imin$
4. $warea \leftarrow \mathbf{sum}(nim \leq imax)$
```

Giving pixels weights according to their shade can be seen as trying to establish a measure of the plume's volume. A darker pixel means more depth, a lighter less depth in the inwards direction of the image. It has to be made clear that there is nothing indicating a linear weighting of pixels. A logarithmic or inverse logarithmic weighting might be a better approach. One could also consider a look-up-table solution which would be suitable for storing and recovering weights in a future implementation of a fully developed algorithm. Algorithm 13 is based on a linear weighting.

6.4.2. Rotated Plume Estimation. Rotating the two dimensional projection of the plume we can approximate the coal particle cloud volume by estimating the plume's body of revolution. The algorithm here might seem a little awkward considering computational efficiency. To start with the mean values for the pixels representing the coal plume are found for both the horizontal and the vertical direction. The covariance matrix and the eigenvalues are calculated. This is done in order to rotate the detected coal particle cloud with such an angle that it is standing upright i.e. the lower end is where the coal comes out of the tuyere, see Figure 6.4.1.

Now we can apply the actual algorithm itself. The mean values for the pixels in the horizontal direction are calculated. The volume of the left part and the right part are calculated separately and then added together to embody the total approximated volume. This is done as an attempt to describe the body of revolution for the plume.

Calculating each half of the coal particle cloud is done in the following way. First the number of pixels in each row on the left side i.e. left of the calculated middle line of the plume, are stored in a vector. Then each value in the vector is treated as a radius of the plume's left half at that particular row. Using these radia we can calculate areas of as many half circles as there are values in the vector. Summing all the areas we obtain a volume for the left half of the pulverised coal cloud. Now the same procedure is applied to the right side of the plume. In the end the two volumes are added to form the final result, the plume's approximated volume. Algorithm 14 illustrates the procedure.

6.4.3. Approximated Shape Estimation. Yet another algorithm for approximating the volume of the pulverised, coal injected at any point in time and seen with the help of cameras, is the algorithm we chose to call Approximated Shape Estimation. Algorithm 15.

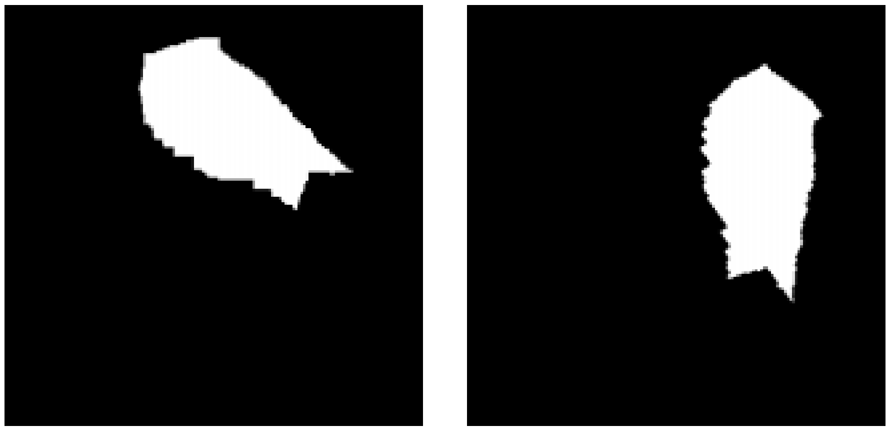

(a) Before. (b) After.

FIGURE 6.4.1. Plume image before and after rotation.

Algorithm 14 Rotalgo

```
rotalgo($im$)
1. $n \leftarrow$ length($im > 0$)
2. $x \leftarrow 0$
3. $y \leftarrow 0$
4. $c \leftarrow 0$
5. $vol \leftarrow 0$
6. for $i \leftarrow 1$ to rows($im$)
7.   for $j \leftarrow 1$ to columns($im$)
8.     if $im[i, j]$ then
9.       $y \leftarrow y + i$
10.      $x \leftarrow x + j$
11.      $c \leftarrow \begin{bmatrix} j \\ i \end{bmatrix} \times \begin{bmatrix} j & i \end{bmatrix} + c$
12.    end
13.  end
14. end
15. $m \leftarrow \frac{\begin{bmatrix} x \\ y \end{bmatrix}}{n}$
16. $cov \leftarrow \frac{c}{n} - m \times m^{tr}$
17. $eigv \leftarrow$ calculate the eigenvalues of $cov$
18. $alpha \leftarrow \frac{180}{\pi} \cdot \arctan\left(\frac{-eigv[2]}{eigv[1]}\right)$
19. $rim \leftarrow$ rotate $im$ by $alpha$
20. $dias \leftarrow$ count the pixels of $rim$ row-wise
21. for $i \leftarrow 1$ to length($dias$)
22.   $vol \leftarrow vol + \pi \cdot \left(\frac{dias(i)}{2}\right)^2$
23. end
```

Algorithm 15 Ellipalgo

```
ellipalgo(im)
1. $minax \leftarrow$ find the minor axis length in $im$
2. $majax \leftarrow$ find the major axis length in $im$
3. $vol \leftarrow \frac{4}{3} \cdot \pi \cdot majax \cdot minax^2$
```

Approximated Shape Estimation is based on the observation of the plume's shape. We could establish that the shape of the projection of the coal particle cloud was very close to elliptic. Now assuming that our three dimensional object is symmetrical along its axes i.e. rugby ball look alike, we can easily compute the volume of such a three dimensional body. Finding both axes' lengths for our projection, computation of the volume is reduced to a straightforward calculation. $volume = \frac{4}{3} \cdot \pi \cdot a^2 \cdot b$, where a is the length of minor axis and b the length of major axis.

CHAPTER 7

Data Extraction and Validation

Image processing had to be used for recovering data from the recorded image sequences. To start with, recorded video signals were digitised according to Chapter 3.4. Performing tests on data from all three data collecting occasions and after some initial stages , have shown similar results on video signals from different tuyeres. We could restrict the final tests to one tuyere from the first and last video recordings. Using the procedures and algorithms developed in Chapter 6, we could extract data from the images. We tried tuyere number 2 from the first and third video recordings, representing two independent data sets, because they had different characteristics. Film sequences were sampled with 2 second intervals and were 600 images long i.e. the studied sampled sequences were 20 minutes long, except for the sequence of Andreas test which consisted of 650 images corresponding to about 22 minutes.

The earlier explained background extracting methods, fixed and customised, were used to find the backgrounds in order to isolate the coal cloud in each picture. The coal cloud was thresholded at eleven different levels, from 0,2 up to 0,7 with step size of 0,05; regarding 0 as the darkest level and 1 as the brightest with 256 grey scale levels in total. From there four algorithms, Area, Imweight, Rotalgo and Ellipalgo, were used for data extraction. Of course we applied all these on each colour buffer. Ending up with $2 \cdot 2 \cdot 11 \cdot 4 \cdot 3 = 528$ different runs. Calculations performed on pictures, as is often the case in image processing, were computationally demanding and time consuming. Today's computers, not the one we used, offer the needed speed. This in combination with an optimised code implementation and suitable choice of programming language, compared to the MATLAB code we used, would boost the data extraction speed in order to allow real-time execution.

Extracted data had to be analysed in a cautious way so that nothing was omitted. Having estimated the coal flow using images, it was close at hand to search for a correlation between our estimation of the flow and different measured signals at the plant.

7.1. Relations Between Algorithms

Having our four algorithms we want to build an opinion about how the algorithms are related to each other. Figure 7.1.1 shows some three-dimensional plots describing the main correlation features according to colour buffers and threshold levels. The colours are running from 1 to 3 and represent red, green and blue respectively. Thresholds are ranging between 1 and 11 from the smallest to the largest. As you can see there are big differences between the two video signals. The left column representing the first video capturing. The Area algorithm shows small correlation with the other algorithms, demonstrating the non-linear relation between them. It is higher for small threshold values due to the fact that the plume is close to non-existent and there is no bigger difference between area and volume estimations. Volume estimation algorithms show high correlation with each other in general. Comparing them using the different background algorithms till shows relatively strong correlation. Figure 7.1.1-(e) reveals the previously mentioned fact that the blue component is not very nice. The customised background tends to get hard to detect, resulting in vanishing plumes while the plumes using the other algorithm are not representative for the coal flow which results in a false strong correlation between them. In this case we have to rely more on the red and green colour buffers.

Moving on to the right column of Figure 7.1.1, we notice that the third video recording is showing some different behaviour. The correlation between area and volume estimation algorithms is weak as expected but uncovers the uneven quality between different threshold levels. Looking at the correlation between the volume algorithms gives high overall correlation but again there are indications of the poor plume quality depending on thresholding level. The lowest threshold levels give no plumes, meanwhile high levels lean toward being fully white; due to overexposure of the video. The good plumes residue somewhere in the middle of the threshold range, where the small correlation dip could otherwise mislead any superficial examiner. Our knowledge of the similarity between the colour buffers in this video signal is confirmed in 7.1.1-(f) in contrast to those in the previously examined video signal. Here we have three useful colours that can be a part of flow estimation algorithms. A good redundancy can be achieved.

7.2. Extracted Data Characteristics

The question now is if the algorithms, applied to the video recordings, give an accurate and representative measurement of the pulverised coal flow.

Close examination has been done on each of the resulting signals after running the different algorithms. This has shown, apart from what we have mentioned about the colour buffer quality and plume thresholding value in Chapter 7.1, that the fixed background gives a better result in general compared to the customised one. This could be related to some bugs in our implementation of the Imconnect algorithm and our badly calculated/estimated threshold values, used in finding the background, in conjunction with not using the best developed algorithm, based on multiple images, for finding the background. The Imweight algorithm proved to be the most suitable among the tested ones, although the other algorithms were not that bad and could be more useful with some modifications. All of the following plots are based on the red buffer of the images, using a fixed background and Imweight for volume estimation at a threshold level of 0,45.

We were lucky to have frequency distorted signals in our first data collecting session, as mentioned in Chapter 4.1. This trait is helpful when looking at the signal dynamics. A quick glance at the frequency content of the measured flow signal and the extracted one shows the same dominant frequency peaks as presented in Figure 7.2.1. The extracted signal is based on fewer samples which gives rougher impression compared to the collected signal but the frequency peak is there at 0,15 Hz. By this we know that we are able to reconstruct the same frequency characteristic of the flow signal with our algorithms. This was a first step in assuring that our measurement was valid.

At a later stage of the project we had to face the fact that the flow measurement quality was not satisfactory. Lack of high correlation is likely due to bad existing measurement. The measured signal is as explained corrected with a correction factor based on the weight signal. This is done because the flow measurement is not good enough to be completely trusted. In this case validation of the extracted data is not an easy task. Searching for the truth we had to look at the other signals related to each tuyere. Those are the pressure and the control signals.

As before both the first and the third video recordings have been inspected and the result is presented in Figure 7.1.1. The left side of the figure, representing the first video signal, is as usual characterised by its frequency content. Best correlation

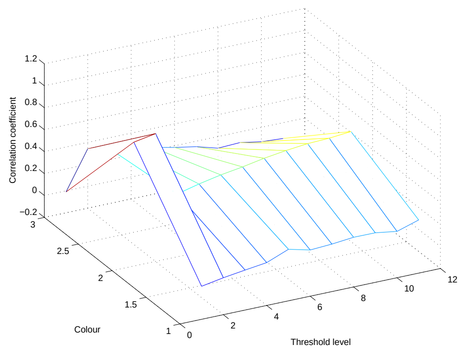

(a) Rotalgo vs. Area, both with fixed background. First recording.

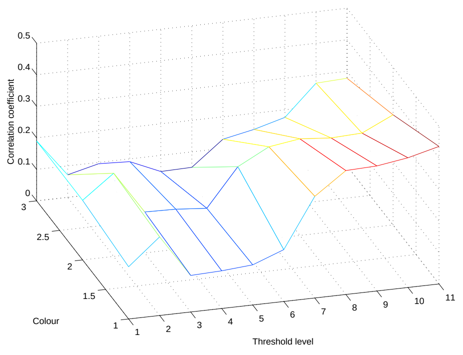

(b) Rotalgo vs. Area, both with fixed background. Third recording.

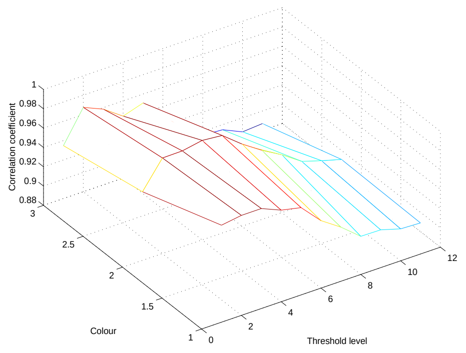

(c) Rotalgo vs. Imweight, both with fixed background. First recording.

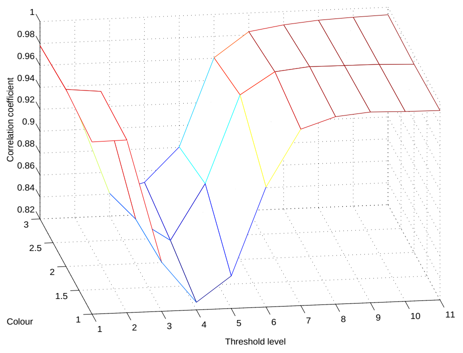

(d) Rotalgo vs. Imweight, both with fixed background. Third recording.

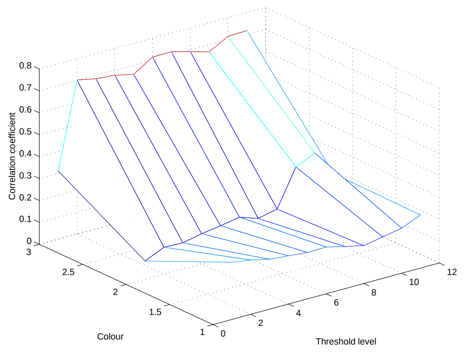

(e) Ellipalgo with customized background vs. Area with fixed background. First recording.

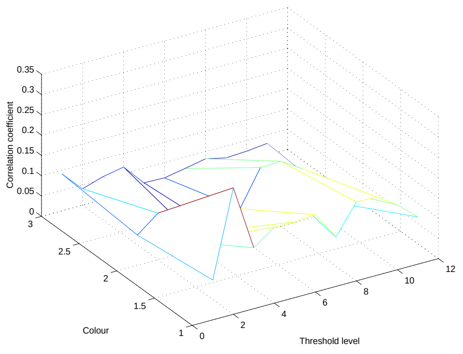

(f) Ellipalgo with customized background vs. Area with fixed background. Third recording.

FIGURE 7.1.1. Correlation between different algorithms.

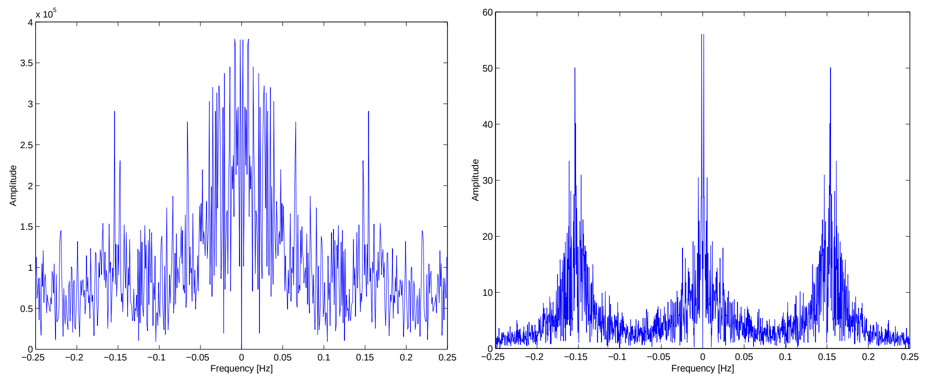

(a) Extracted flow signal. (b) Collected flow signal.

FIGURE 7.2.1. FFT of the extracted flow signal and the collected flow signal.

is obtained with the control signal and the worst one is found with the flow signal measurement. The right side of the figure, representing the third video signal, shows exactly the same trends except for the absence of the “Mefos carrier-frequency” which is not present in the collected signals on this occasion and also the time delays differ. The delay was found to be very small, a few seconds at the most.

Our flow estimation is delayed by approximately 11-13 seconds compared to the control signal. The pressure on the other hand proceeds our extracted data by 9-11 seconds. As a result the correlation peak differs by 2 seconds between he pressure and the control signal. Comparing Figure 7.2.2-(a) nd (b) with Figure 4.1.5-(c) and (d) we notice that there is no clear negative correlation present in the first ones, that is because our flow estimation has no direct feedback to the controller. When it comes to the flow signals correlated with our estimated flow we see a clear difference in the flow measurement quality. In the first recording we can register the flow 3 seconds before the flowmeter, while in the third recording we can do the same 9 seconds before the flowmeter. The negative correlation could be related to the different delays for the control-flow and control-estimated flow, the difference between them is approximately the maximum value in the first minus the maximum value in the second which is about 13 seconds.

Applying the filter identified in Chapter 4.1.1 to the flow signal, from the third video recording and correlating it with the extracted flow measurement resulted in the plot in Figure 7.2.3. he positive correlation noticed in Figure 7.2.2-(f) has increased and moved from -9 to 9 seconds, because of the filter influence. Also we can clearly see a suppression in the negative correlation we had at 13 seconds. This makes the correlation plot look much more similar to those in Figure7.2.2-(b) nd Figure 7.2.2-(d). The good job done by the filter should not be overestimated, remembering that filtering followed by inverse filtering can distort the signal. This could be noticed because the signal fluctuates with higher frequency as Figure 4.1.6 shows.

Data was filtered using different low-pass filters to get rid of the high frequency fluctuations consisting of pure noise. This was mainly visible in the algorithms using a customised background approach. Now the correlation, not very surprisingly, increased slightly to reach above 0,5. Unfortunately, for a closer validation we would need to know the exact amount of coal injected at any time. However, for

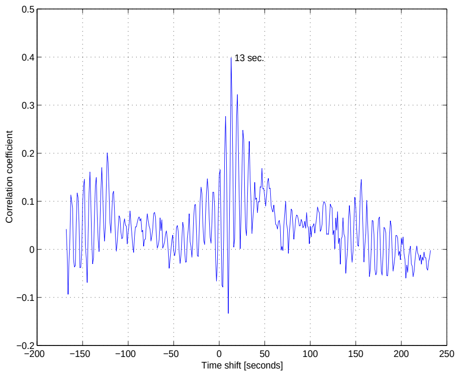

(a) With control signal. First recording.

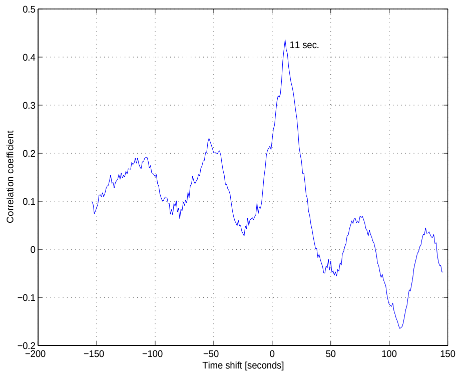

(b) With control signal. Third recording.

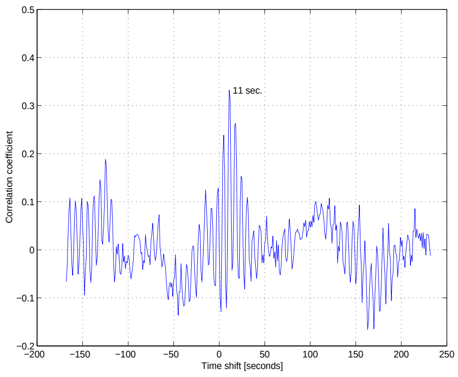

(c) With pressure signal. First recording.

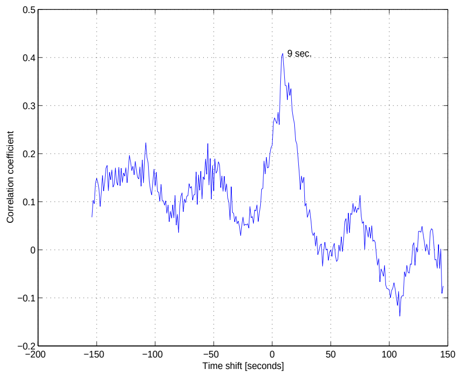

(d) With pressure signal. Third recording.

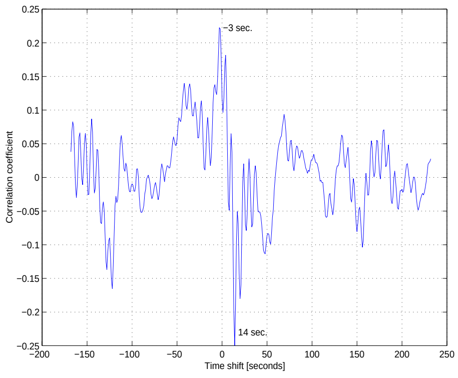

(e) With flow signal. First recording.

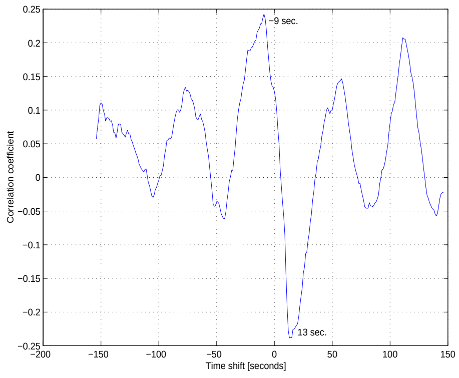

(f) With flow signal. Third recording.

FIGURE 7.2.2. Correlation between the extracted flow signal and different measured signals.

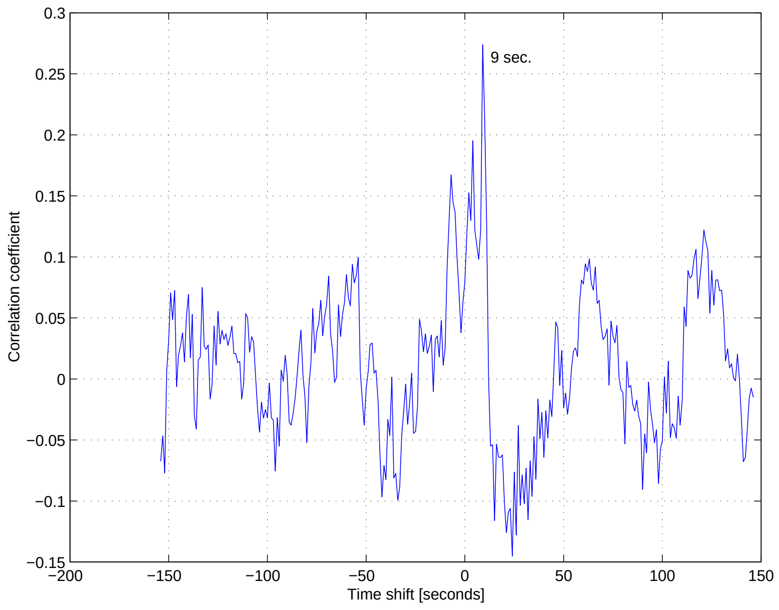

FIGURE 7.2.3. Correlation between the extracted flow signal and the filtered flow signal, from the third video recording.

now we were looking forward to see a higher correlation with the current data. Here we have a problem since we know that the current measurement can not be trusted and the other measured data are related to the flow measurement. A warning finger should be raised whenever there is slag injected together with coal, because then the flowmeters really misbehave and do not serve their purpose any good. Slag and coal powder can not be separated in our images, with the current quality. We have only seen slag injected from behind a green glass.

7.3. Andreas Test Properties

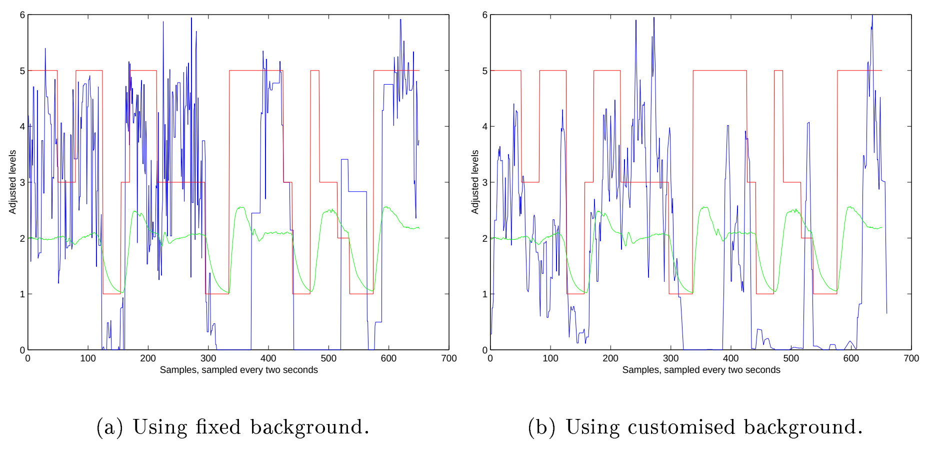

(a) Using fixed background. (b) Using customised background.

FIGURE 7.3.1. A comparison between valve position signal (red) , flow signal (green) and extracted flow signal (blue) during Andreas test.

Another test was made to check if choking the flow could be noticed in the data extracted from the film sequence, see Figure 7.3.1 for a simple comparison. Both the fixed and customised backgrounds follow the valve position roughly, and so does the flow signal. We can see that the customised background fails slightly when the valve is totally closed. On the other hand we can see that the customised background based algorithm behaves in the same way, as the valve position signal, during the third and fourth valve closings; in contrast to the fixed background based algorithm which shows different behaviour.

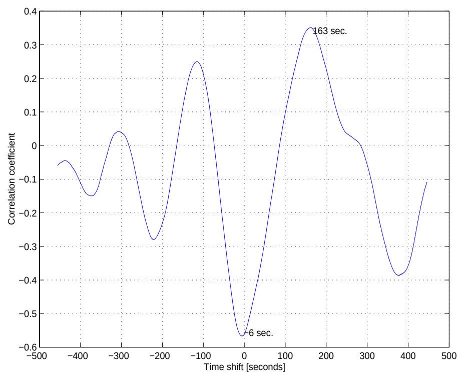

(a) With control signal.

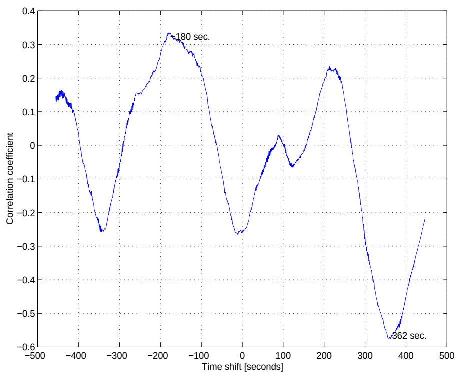

(b) With pressure signal.

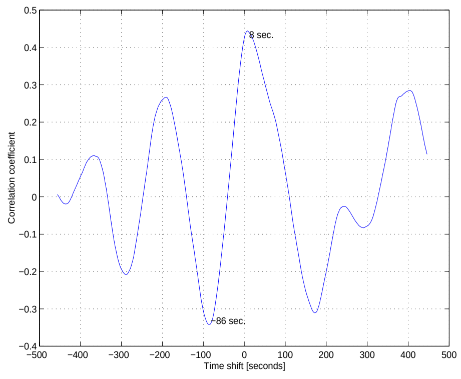

(c) With flow signal.

Figure 7.3.2. Correlation between the extracted flow signal and different measured signals during Andreas test.

We found it suitable to highlight the correlation between the collected signals and the extracted one during the Andreas test, as we did before for the other video sequences. Because the valve closing takes place on different valves that are placed differently, relative to the measurement device, we will have different plots compared with those we got earlier. As Figure 7.3.2 illustrates, the correlation with the control signal is strongly negative at -6 seconds, that is a delay of 6 seconds in the control signal after an action of closing or opening has been taken.

Looking further into the properties of the pressure signal, no particular correlation can be found. This does not surprise however since we know that choking the coal flow after the pressuremeter will result in increased pressure while doing

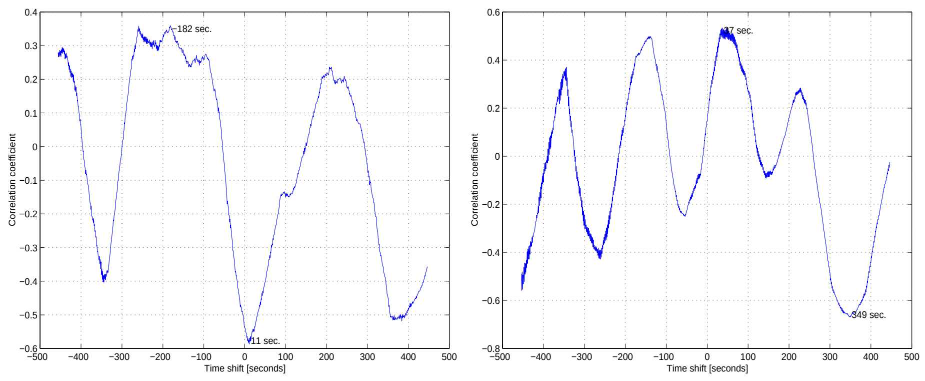

(a) The valve after the pressure meter. (b) The valve before the pressure meter.

Figure 7.3.3. Correlation between the extracted flow signal and the pressure signal during Andreas test.

the same before the pressuremeter will decrease it, whereas the flow will always decrease. In this case we need to separate the Andreas test into two cases which are outlined in Figure 7.3.3. The first, shutting of the flow after the meter, gave a strong negative correlation with 11 seconds delay before we discovered that something had happened in our images. The second, where shutting of the flow was before the meter, led to a positive correlation after 37 seconds. Seemingly, the difference in the delay time is simply depending on the distance the coal has to travel, before reaching the tuyere's mouth and get on the tape, but we still think it is too long.

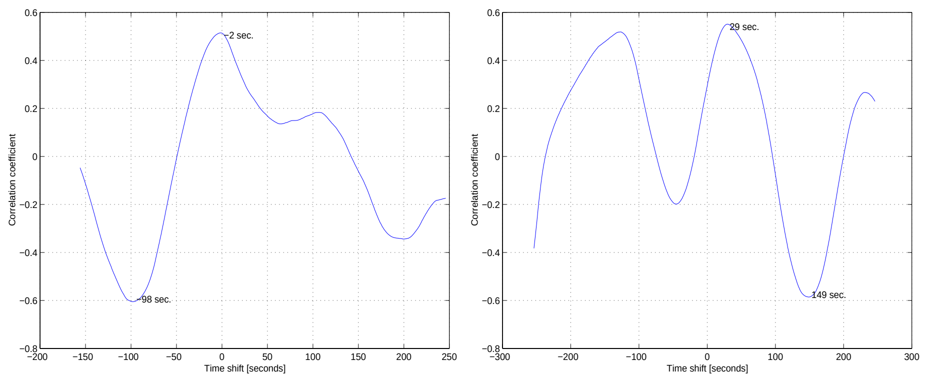

(a) The valve after the flow meter. (b) The valve before the flow meter.

Figure 7.3.4. Correlation between the extracted flow signal and the flow during Andreas test.

Lastly we will, without being inconvenient, torture the flow measurement and see f it will confess. Figure 7.3.2-(d) shows a positive correlation at 9 seconds which conflicts with our previous result of -9 seconds. Again here we had a reason to separate the extracted signal in two parts. This has increased the correlation in general. Plot (a) in Figure 7.3.4 gave us a delay of -2 seconds implying that we are able to detect the changes in the coal flow before the meter does. The meter seems to continue measuring the flow for a while after the actual flow cut off. On the contrary plot (b) in the same figure tell us that the correlation maximum occurs at 29 seconds. Now the flowmeter is faster than our calculated flow. We guess that the flowmeter is very dependent on the carrier medium.

CHAPTER 8

Conclusions and Suggestions

Image processing has hopefully proven to be an asset amongst other tools that can be used for enhancing the monitoring of the blast furnace process. This is quite a new research area which most probably will eventually lead to an improved surveillance and control of the process. What is described in this report is a first reach for utilising computer vision systems in steel making industry by monitoring process parameters. To round off this report we will briefly present some conclusions and then discuss a few suggestions for potential improvements and further work to be done.

8.1. Conclusions

Studying the whole process and developing algorithms based on image processing for watching the process' behaviour, we came up with some conclusions. They are all gathered here.

First, we can say that the current flow measurement is not satisfactory or at least it could be improved using image processing. This statement is based partly on what we have been told at Mefos but mostly on what we discovered comparing data extracted using image processing to the collected flow signals. There should be a high correlation between those which could not be found. We could only detect a lower degree of correlation. Since this was quite a surprising result further tests were made. In one of these the coal flow was choked and later the measured flow examined. Our algorithms could detect changes in the coal flow. We tried also to correlate the estimated volume to the control signal, the correlation increased. Another, less sophisticated way of seeing that the present flow measurement is not very reliable was to simply find a film sequence where we saw that the flow was low in the beginning and high towards the end. We also knew that the camera was not moved or zoomed during filming time. Now, the present flow measurement did not change at all whereas data recovered from images indicated the observed rise in coal particle flow. Unless coal flow suddenly changed path, right after injection to the blast furnace, the current coal flow measurement is inadequate. The missing link here is still a conversion between calculated volume and useful flow measurement.

Another conclusion was that using the green glass, as a protecting filter for the cameras, skews the colour buffers, specially the blue one. Since the cameras are colour cameras, we lose valuable information in one of the channels. The red and green buffers look decent despite the just mentioned filter. But of course all information is valuable so being able to use the blue buffer as well as the two others would be advisable.

Still investigating the cameras, we can state that if image processing is to be applied, not making it too complicated, a static image is needed. Algorithms have been developed to avoid this problem and those are comparable with the assumption of static images. An additional obstacle is that the plume is filmed from an angle. This makes it slightly harder to estimate the volume of it. Strict camera positions have to be used in order to be able to rotate the plume and calculate its exact volume.

Looking into the future, not only do we want to estimate the coal flow but also study other process parameters. For this a good resolution and adjustment of cameras is of great importance. Image processing algorithms must be working in real-time, which could demand quite a lot of computational power, especially if the number of tuyeres is large. It would though certainly be an investment that pays off in the future.

8.2. Suggestions

Having discussed all encountered problems it would be nice to give some answers. These suggestions might be technically very hard to achieve but nevertheless complaining about things in the existing plant we owe some suggestions for improvements.

First of all, the flow measurement should be improved using image processing. Image processing could even be used alone in the future, providing efficient and reliable image processing algorithms are fully developed. A closer study of the behaviour of the pulverised coal in the pipes could also be enlightening. It would for sure, to some extent, help understanding how the flow should be measured. Other changes to be made in order to make the image processing and calculations involved as simple as possible are mostly concerning the cameras.

The green glass filter in front of each camera should be replaced by a transparent filter that lowers the intensity of light but does not distort it in any way. Doing that we will gain a set of three channels with information, which as mentioned would be good for redundancy reasons and at the same time do not expose cameras to excessive light.

When it comes to video recording synchronisation, a good synchronisation signal should be created if delays have to be determined with great accuracy. This should trig the cameras/VCRs and the data acquisition box. An external trig signal is preferred. Using the same trig signal to initiate grabbing is a good idea.

It is a good idea to change Andreas test from closing valves to changing the setup value of the coal powder flow. This is easier to change and more sensitive to small changes. Changing the setup value in a manner that guarantees different transitions between low-high flows, will improve the test, keeping in mind that the changes have to be held for periods longer than the system delays.

As we discussed before a static picture makes analysis less complicated. Therefore cameras should be zoomed on the interesting area of the picture and then mounted in some way so this picture remains static during the whole time we are interested in surveilling coal injection. If the cameras were fixed, as well as other movable parts like the tuyeres also the task of compensating for the angle from which the plume is seen would be a one-time calculation. When the angles of the cameras can be changed, they can be moved backward and forward, and the tuyeres are not fixed, then we have a situation where the angle from which the plume is seen is constantly changing, which of course does not make life any easier.

A somewhat different problem to be solved, concerning cameras used for coal powder surveillance, is that most cameras auto-adjust to current conditions. This means that a camera is constantly adjusting depending on the amount of coal present in the image due to noticeable changes in brightness. This phenomenon will evidently harm a measurement of temperature which is highly dependent on colours being compared between two different frames. It could also harm the coal flow estimation. Having a fixed colour reference is valuable. Even when no real changes occur in the colour of the flame, an auto adjusting camera could perceive two different colours. A remedy for this is, if possible, disallowing auto adjustment.

Shutter time has to be constant and no changes made to the lens aperture while in operation.

Further if we are to do all computations needed in real-time, the most feasible solution is using digital cameras to avoid distortions in image quality by eliminating digitising and sampling effects. It is of great help when comes to squashing the time needed to produce useful data from images. 12-bit cameras, which have appeared on the market, could enhance the resolution and using several cameras for each tuyere would allow a more accurate measurement of the volume of the coal particle cloud. More than one camera for each tuyere will complicate the problem, therefore it is advisable to improve the algorithm developed for one camera unless a more exact coal estimation is needed.

Finding a functional model for the coal cloud behaviour would contribute to enhancing the coal flow measurement as well. A good model for the plume/flame would be of great help. Having a good volume estimation is essential.

A closer investigation of what exactly happens when slag is injected, besides pure coal powder, is advised. Slag injection makes the whole injection process even more complicated. The case when slag is injected with coal should be studied and compared to the pure coal injection.

Bibliography

[1] *Agarwal, Jay; Brown, Francis; Chin, David (1996).* The future supply of coke. New Steel [H.W. Wilson - AST], vol. 12, p. 88. ISSN 1074-1690.

[2] *Birk, Wolfgang (1997).* Pressure and flow control of a pulverized coal injection vessel. Sweden: Luleå University of Technology. Master thesis/1997:045, . 38-41. ISSN 1402-1617.

[3] *Creek, Patricia; Moccia, Don (1996).* Digital media programming guide. Silicon Graphics Inc. Document Number 007-1799-060. URL: http://autarch.loni.ucla.edu/ebt-bin/nph-dweb/dynaweb/SGI_Developer/DMediaDev_PG/@Generic__BookTextView/3;cs=fullhtml;pt=4

[4] *Daoud, Jihad; Durand, Cyril; Mock, Nico; Nipl, Igor; Sayyahfar, Zohreh (1999).* Optimazation of washing control at AssiDomän Kraftliner in Piteå. Sweden: Luleå University of Technology. Automatic control project.

[5] *Jain, Anil K. (1989).* Fundamentals of digital image processing. USA: Pentice-Hall, Inc. ISBN 0-13-332578-4.

[6] *Johansson, Andreas (1999).* Model-based leakage detection in a pressurized system. Sweden: Luleå University of Technology. Licentiate thesis 1999:37. ISSN 1402-1757.

[7] *Lorenz, Juergen (1999).* CVC Color - Software tool for color recognition. Stemmer Imaging GmbH. URL: http://www.cvc-imaging.com/Cvc_Tools/Bildverarbeitung/Color/Farbmodelle_e.htm

[8] *Low, Adrian (1991).* Introductory Computer vision and image processing. England: McGraw-Hill Book Company (UK) Ltd. ISBN 0-07-707403-3.

[9] *Matrox Image Processing group (1998).* Matrox Meteor - Installation and hardware reference. Canada: Matrox Electronic systems Ltd. Manual No. 10529-MT-0110.

[10] *McManus, George J. (1994).* Replacing coke with pulverized coal. Iron Age New Steel, New York, vol. 10, issue 6, p. 40. ISSN 1074-1690.

[11] *O'Hanlon, J. (1993).* Injection of granular coal into the blast furnace. Steel Times vol. 221, issue 12, p. 508-509. ISSN 0039-095X. CODEN STLTA3.

[12] *Ondrey, Gerald; Parkinson, Gerald; Moore, Stephen (1995).* Blast furnaces make way for new steel technology. Chemical Engineering [H.W. Wilson - AST], vol. 102, p. 37. ISSN 0009-2460.

[13] *Oshnock, T.W. (1995).* Pulverized coal injection for blast furnace operation. Iron & Steelmaker (I&SM) vol. 22, issue 4, p. 49-50. ISSN 0275-8687.

[14] *Piersol, Bendat (1971).* Random data: Analysis and measurement procedures. USA: John Wiley & Sons, Inc. ISBN 0-471-06470-X.

[15] *Porat, Boaz (1996).* A course in digital signal processing. UK: John Wiley &Sons, Inc. ISBN 0-471-14961-6.

[16] *Ramsey Technology, inc. (1996).* Installation & operation manual for Ramsey DMK 270 transmitter with Granucor. REC 3956, REV B 10/96, PART NO. 050622.

[17] *Tottie, Magnus (1999).* LKAB's Experimental Blast Furnace at MEFOS/Luleå.
URL: http://www.lkab.se/english/company/mt/pilot_mt_english.html (1999-06-24).

APPENDIX A

MATLAB Code

A.1. mam.m

```
% Purpose:
% Get the largest element, independent of the matrix dimension.
%Synopsis:
% m = mam(x);
%Description:
% First establish the dimension of X and then get the largest
% element in it.
%See also:
% MAX, MIN

function m = mam(x);

= length(size(x));
m = x;
for i = 1:d
m = max(m);

end
```

A.2. mip.m

```
%Purpose:
% Get the smallest element in a 2-D matrix and return its position.
%Synopsis:
% [v, r, c] = mip(x);
%Description:
% First the smallest element the matrix and then calculate its position.
%See also:
% MAM, MAX, MIN

function [v, r, c]=mip(x);

[v a] = min(x);
[v c] = min(v);

r = a(c);
```

A.3. imframe.m

```
%Purpose:
% Make the image boundary black.
%Synopsis:
% j = imframe(i,s)
%Description:
% If 2*s+1 is smaller than the number of columns and rows of the
% image then j is the same images as i with a black s-pixels boundary.
%See also:
%
function j = imframe(i,s);
[r,c] = size(i);
if (r<2*s|c<2*s)
 error('''2*s'' should be smaller than the image size in each direction');
end
j=zeros(r,c);
(s+1:r-s,s+1:c-s)=i(s+1:r-s,s+1:c-s);
```

A.4. imends.m

```
%Purpose:
% Find the end pixels in an binary images.
%Synopsis:
% [e,v,u]=imends(i)
%Description:
```

```
% An end in a binary image is a pixel connected with at most one
% other pixel, to the neighbouring 8 pixels.  e is a vector of
% pixels order, u is describing which line segment each pixel
% belong to, and v is the direction in which way they are connected
% as it is described below (zero means no connection), as you may
% imagine we assume thin line segments:
% 1 2 3
% 4 0 5
% 6 7 8
%See also:
% IMCHAIN, IMFILTER

function [e,v,u]=imends(i)

[r,c]=size(i);
i1=zeros(r+2,c+2);
i1(2:r+1,2:c+1)=i;
[r1,c1]=find(i1);
p=[07 11 13;
  17 00 19;
  23 29 31];
=sort(reshape(p,9,1)');
%This l below is if you don't want to treat single points as end
%points.  Comment it if you don't like it and don't forget to change
%v=[v y] into v=[v y-1] below.
%l=l(2:9);
e=[];
v=[];
n=i1;
w=1;
wx=[];
u=[];
for x=1:length(r1),
  a=r1(x);
  b=c1(x);
  d=i1(a-1:a+1,b-1:b+1);
en=n(a-1:a+1,b-1:b+1);
 y=unique(en(find(en>1)));
 f sum(max(y)*ones(size(y))-y)
     up=[];
     down=[];
     for ij=1:length(y)
       down=[down (find(n==y(ij)))' ];
     end
   n(down)=max(y);
     if length(u)
       for ij=1:length(y)
       up=[up find(u==y(ij))];
        end
       u(up)=max(y);
     end
   end
mn=mam(en);
  if mn==1
   w=w+1;
   mn=w;
  end;
na-1:a+1,b-1:b+1)=(n(a-1:a+1,b-1:b+1)&ones(3))*mn;
 s=sum(sum(d.*p));
y=find(l==s);
  if y
   if length(wx)<mn
     wx(mn)=0;
   end
wx(mn)= wx(mn)+1;
   e=[e x];
   v=[v y-1];
   %v=[v y];
   u=[u mn];
  end

end
```

A.5. line2pixel.m

```
%Purpose:
% Convert lines, described by two end points, into pixel(s) in an
% image or elements in a matrix.
%Synopsis:
```

```
% [r,c]=line2pixel(x,y)
%Description:
% Found the pixels below a line and return thiere positions.
% Don't worry about any warning like "Warning:  Divide by zero.", it
% has been taken care of.
%See also:
% CAPTURE, ROIPOLY

function [r,c]=line2pixel(x,y)

warning off;
r=[];
c=[];

i=2:2:length(x);
j=i-1;
x1=x(j);
x2=x(i);
y1=y(j);
y2=y(i);
=(y1-y2)./(x1-x2);
b=y2-m.*x2;
for p=1:length(b)
  s=x1(p);
  t=x2(p);
  u=y1(p);
  v=y2(p);
  if u<v
   r1=u+1:v-1;
  elseif u>v
   r1=v+1:u-1;
  else
   r1=[];
  end
  if s<t
   c1=s+1:t-1;
  elseif s>t
   c1=t+1:s-1;
  else
   c1=[];
  end

if isempty(c1)
c1=s*ones(size(r1));
elseif isempty(r1)
r1=u*ones(size(c1));
  else
 c2=round((r1-b(p))/m(p));
 r2=round(m(p)*c1+b(p));
   c1=[c2 c1];
   r1=[r1 r2];
  end
  c=[c c1];
  r=[r r1];

end
```

A.6. imconnect.m

```
%Purpose:
% Connect discontinuous edges or pixels in a binary image.
%Synopsis:
% j=imconnect(i)
%Description:
% Find the discontinuous parts using imends and then connect the
% parts in a minimum way.  j is the new edge connected image.
%See also:
% IMENDS, IMCHAIN
function j=imconnect(i)
%When you are in trouble, you need at least two objects in the image to connect!
%(:,round(length(i)/2))=0;
%(round(size(i,1)/2),:)=0;
[e,v,u]=imends(i);
% Remember that all the endpoints are not real endpoints!
[r,c]=find(i);
% d is the distance matrix between the endpoints.
for z=1:length(e)
()sqrt((r(e)-r(e(z))).^2+(c(e)-c(e(z))).^2);
end
```

```
u1=u;
count=zeros(1,max(u));
losers=[];
dfind(d==0))=mam(d)+1;
m=1:length(e);
on=zeros(1,length(e));
sel=[];
w=[];
ines=length(unique(u));
done=0;
while find(con==0)
 m1=setdiff(m,union(sel,losers));
  bad=1;
if isempty(m1)
   break;
  end
  while bad
[v1,r1,c1]=mip(d(m1,m1));
   x1=m1(r1);
   x2=m1(c1);
%if length(find(con==0))==2
if length(unique(u))==1
     ok=0;
         %%%%% bad=0;
     % the next two rows is used if you want to connect every end
     % in the last segment!
   %ucount(u1(x1))=ucount(u1(x1))+1;
   %ucount(u1(x2))=ucount(u1(x2))+1;
   else
   ok=u(x1)==u(x2);
   end
   if ok
     m2=setdiff(m1,x1);
     if isempty(m2)
                break;
     end
   [v1,r1,c1]=mip(d(m2,m2));
     m3=setdiff(m1,x2);
   [v2,r2,c2]=mip(d(m3,m3));
     if v1<v2
                m1=m2;
     else
                m1=m3;
     end
   else
     bad=0;
   end
  end
w=[w x1 x2];
 ucount(u1(x1))=ucount(u1(x1))+1;
 ucount(u1(x2))=ucount(u1(x2))+1;
if ucount(u1(x1))==2
   losers=[losers find(u1==u1(x1))];
  end;
if ucount(u1(x2))==2
   losers=[losers find(u1==u1(x2))];
  end;
  if (lines-done)~=2
up=find(u==u(x1));
u(up)=u(x2);
  end
  done=done+1;
if ~con(x1)
   if v(x1)
     con(x1)=1;
   else
     v(x1)=9;
   end
  end
if ~con(x2)
   if v(x2)
     con(x2)=1;
   else
     v(x2)=9;
   end
  end
sel=find(con);
end
,]=line2pixel(r(e(w)),c(e(w)));
```

```
ull(sparse(y,x,ones(size(x)),size(i,1),size(i,2))) | i;
```

A.7. imfilter.m

```
%Purpose:
% Filter out isolated pixels in an image.
%Synopsis:
% f=imfilter(i,y)
%Description:
% The binary image p is converted into double, if needed, and the image
% will be scanned with a y-by-y square that filter out isolated spots
% according to y.  y is the sized of isolated spots.
%See also:
% FILTER2, BWMORPH, IMREG

function f=imfilter(i,y);

f isa(i, 'uint8')
i = double(i);
end
[m,n]=size(i);
for d=1:length(y)
x=y(d);
f=zeros(m+2*x,n+2*x);
f(x+1:m+x,x+1:n+x)=i;
[c,r,v]=find(f);
x0=ones(2*x+1);
  x0(2:2*x,2:2*x)=0;
for j=1:length(c)
   ci=c(j);
   ri=r(j);
i-x:ci+x,ri-x:ri+x)=~(sum(sum(f(ci-x:ci+x,ri-x:ri+x).*x0))==0).*f(ci-x:ci+x,ri-x:ri+x);
  end
i=f(x+1:m+x,x+1:n+x);
end
f=i;
```

A.8. imback.m

```
%Purpose:
% Get an image background and make it black.
%Synopsis:
% bg=imback(i)
%Description:
% bg is a binary image where the black part represent the
% background and the white is, off course, the foreground.  The
% parameter t is the threshold used to detect the background
% edges.
%See also:
% BWMORPH, IMCONNECT, BWFILL, EDGE

function bg = imback(i, t);

%Try to Find the optimal threshold for each image, image type,
%it is more accurate than any imthresh based on the mean value and/or
%the standard deviation of the image.  This seems to be true at
%least for the stupid blue image we have!
e = edge(i, '', t);
j = imframe(e, 5);
%A better imconnect could eliminate the next step.  The goal of this
%is to get a thin edge, one pixel wide with no glitches!
bwmorph(bwmorph(j, 'dilate', 2), 'shrink', 3);
% adjust this due to what trash you want to clean, "3" is good for
% getting rid of "single" pixels.
%f=imfilter(b, 3);
c = imconnect(b);
g = bwfill(c, 'holes');
```

A.9. dyncrop.m

```
%Purpose:
% Find the interesting area in an image and crop it.
%Synopsis:
% [i, x, y, r, c] = dyncrop(im)
%Description:
% Based on the standard deviation and the mean value of
% an image and where the light area are present the image
% is cropped and its crop parameters are returned.  i is
% the cropped image, x and y are the start positions,
% r and c are the dimensions of the cropped area.
%See also:
% IMCROP

function [i, x, y, c, r] = dyncrop(im)

%Find where the interesting area is
xs = sum(im);
ys = sum(im');
m = mean(xs)-std(xs)/2;
m = mean(ys)-std(ys)*2/3;
xf = find(xs>xm);
yf = find(ys>ym);
x = min(xf);
x2 = max(xf);
y = min(yf);
y2 = max(yf);
c = x2-x;
r = y2-y
i = imcrop(im, [x y c r]);
```

A.10. dynbg.m

```
%Purpose:
% Find the image background.
%Synopsis:
% bg = dynbg(im, th)
%Description:
% First find the interesting area in the image, then do some
% edge detection and morphological operations.
%See also:
% DYNCROP, IMBACK

function [bg, x, y, c, r] = dynbg(im, th)

fim = medfilt2(im);
%Find where the interesting area is
[fim, x, y, c, r] = dyncrop(fim);
if nargin==1
fim = edge(fim, '', (255-mean2(fim))*4/7/255);
else
fim = edge(fim, '', th);
end
= bwmorph(bwmorph(fim, 'dilate', 2), 'shrink', 3);
fim = imconnect(fim);
im = bwfill(fim, 'holes');
```

A.11. bgmulti.m

```
%Purpose:
% Find the background in an image.
%Synopsis:
% y = bgmulti(im, s, n, c, layer, accept)
%Description:
% Find the background in a series of images based on several
% consecutive images.  im is the image series, s is the start
% point, n is the number of images to detect their background
% and c is the wanted color layer.  layer is the number of
% consecutive images to use and accept is the threshold for
% edge acceptance which is less than or equal to layer.
%See also:
% IMBACK,

function y = bgmulti(im, s, n, c, layer, accept)

ok = 0;
for i = 0:n-1
   while ok < layer
   e(:, :, ok+1) = edge(im{s+ok+i}(:,:,c), '', (255-mean2(im{s+ok+i}(:,:,c)))/2/255);
      ok = ok + 1;
   end
  tmp = sum(e,3)>(accept-1);
 {s+i}(:, :, c) = bwmorph(bwmorph(tmp, 'dilate', 5), 'thin', inf);
  ok = ok - 1;
   for j = 1:ok
```

```
    e(:, :, j) = e(:, :, j+1);
   end

end
```

A.12. imarea.m

```
%Purpose:
% Calculate the weighted area in an image.
%Synopsis:
% a = imarea(i);
%Description:
% A dark pixel have a higher weight than a light pixel.  Given an
% intensity image the maximum and minimum intensity values (!= 0)
% are calculated and the pixels values are re-mapped to reflect
% their weight.  The result is the sum of the weighted pixels.
%See also:
% BWAREA

function a = imarea(i);

[n, m] = size(i);
r = reshape(i, n * m, 1);
[x, y, v] = find(r);
i1=0;
if ~isempty(v)
  vmin = min(v);
  vmax = max(v);
i1 = double(i) - double(vmin);
  l = find(i1 < 0);
  i1 = double(vmax) - i1;
   i1(l) = 0;
end

= sum(sum(i1));
```

A.13. algox.m

```
%Purpose:
% Clean up in an BW-image, from uninteresting objects.
%Synopsis:
res = algox(im, th, xc ,yc)
%Description:
% Identify the objects in the image and see which object is closest
% to the given point (xc, yc).  th is used to get rid of small
% object, it is simply the number of white pixels in those objects.
%See also:
% BWMORPH

unction res = algox(im, th, xc ,yc)

im = bwlabel(im);
a = max(max(im));
r = [];
if ma > 1
   for i = 1:ma
      tmp = im==i;
     s = sum(sum(tmp));
      if s < th
        im(tmp)=0;
      else
        [y, x] = find(tmp);
        xt = mean(x);
        yt = mean(y);
      r(i) = sqrt((yt-yc)^2+(xt-xc)^2);
      end
   end
  if length(r) > 0
     r(find(r==0)) = 1000;
     [v, o] = min(r);
      res = (im == o);
   else
      res = im;
   end
else
   res = im;

end
```

A.14. findflame.m

```
%Purpose:
% Find flame in a picture, when the background is available but the
% interesting region in the image is unknown.
%Synopsis:
% flame=findflame(im,mask,th1,th2)
%Description:
% Given an image, a background mask (smaller than the image) and
% threshold values it is possible to a flame in the picture.th1 is
% the value used to threshold for the flame and th2 is used to
% position the mask on the image.
%See also:
% IMFLAME

function out=findflame(im,mask,th1,th2)

[I1,J1]=size(mask);
im=double(im)>th1;
i=find(sum(im')>th2);
j=find(sum(im)>th2);
iround((max(vi)+min(vi))/2);
jround((max(vj)+min(vj))/2);
ri=im(i-I1/2:i+I1/2-1,j-J1/2:j+J1/2-1);

out=(1-roi).*mask;
```

A.15. imflame.m

```
%Purpose:
% Find a certain intensity level, representing the flame.
%Synopsis:
% l = imflame(I, th, BG, x, y);
%Description:
% The background, BG, image is subtracted from the image I after
% thresholding at th, where th is 0.0-1.0.  The resulting image is
% modified and cleaned with some morphological operation.  x and y
% represent the end of the tuyere where the coal is spread out.
%See also:
% EDGE, IM2BW, BWMORPH, FINDFLAME

function l = imflame(I, th, BG, x, y);

l= double(BG)-double(im2bw(I, th));
bwmorph(bwmorph(l>0,'erode',2),'dilate',2);

l = algox(l, 200, x, y);
```

A.16. algo2vol.m

```
%Purpose:
% Calculate the approximate volume of a 2-D coal particle cloud.
%Synopsis:
% v=algo2vol(plym)
%Description:
% Assuming that the projection of the plume is always oval we can use a
% simple algorithm for calculation of the volume.  All we need is the length
% and the width of the plume.
% a is the width of the plume
% b is the length of the plume
%See also:
% IMFEATURE

function volume=algo2vol(plym)

[x,y]=find(plym);
if x>0
  master=imfeature(plym,'MinorAxisLength');
   a=master.MinorAxisLength;
  master=imfeature(plym,'MajorAxisLength');
   b=master.MajorAxisLength;
   area=pi*a*b;
   volume=4*area*a/3;
else
   volume=0;

end
```

A.17. evalvol.m

```
%Purpose:
% Evaluation of volume given a vector of radia.
%Synopsis:
% v=evalvol(vector)
%Description:
% Find the volume of half circles given their radia in a vector.  Then add
% all these values together to get an approximate volume for one half of
% the body of revolution.
%See also:
% COUNTPIXELS, FINDVOLUME2

function vol=evalvol(vector)

vol=0;
for n=1:length(vector)
  vol=vol+(pi*vector(n)^2)/2;
end;
```

A.18. countpixels.m

```
%Purpose:
% Count the on pixels in every row of an image and store the result as
% numbers in a vector.
%Synopsis:
% vector=countpixels(plym,begincolumn,endcolumn)
%Description:
% Given a binary image of a plume, the beginning and the end columns
% for which we want the calculation to be performed a vector of number of
% on pixels in each row between these two columns is calculated.
% If no start or end values are given, calculation is performed
% for the whole length of the horizontal-axis.
%See also:
% EVALVOL, FINDVOLUME2

function vector=countpixels(plym,b,e)

[r, c]=size(plym);
if nargin==1
   b=1;e=c;
end
if r==0
   r=1;
end
if e==0
   vector=0;
else
   for l=1:r
   vector(l)=length(find(plym(l,b:e)==1));
   end
end
```

A.19. findvolume2.m

```
%Purpose:
% Calculate the approximate volume of a 2-D coal particle cloud using the
% rotation algorithm.
%Synopsis:
% v=findvolume2(plym)
%Description:
% Find the volume of a particle cloud using countpixels and evalvol.  To start
% with the mean values for the on pixels are found for both horizontal and
% vertical direction.The covariance matrix is calculated and then the
% eigenvalues for it.  This is done in order to rotate the plume with such
% an angle that it is standing upright i.e.  the bottom end is where it
% comes out of the tuyere.
% Now the algorithm can be applied on the plume.  The mean for the on pixels
% is calculated for the horizontal direction.  When this is done the volume
% volume of the left part and the right part are calculated separately using
% the functions countpixels and then evalvol.
%See also:
% COUNTPIXELS, EVALVOL, COV, EIG

function volume=findvolume2(bwplymim)

[ycoord,xcoord]=find(bwplymim);
```

```
if length(ycoord)>0
   v=[ycoord xcoord];
  m=mean(v);
  c=cov(ycoord,xcoord);
  [v,d]=eig(c);
alpha=180*atan(-v(1,2)/v(1,1))/pi;
  rotated=imrotate(bwplymim,-alpha,'crop')>0;
  [i,j]=find(rotated);
  im=mean(i);jm=mean(j);
  rotax=round(jm);
   if rotax>0
     left=countpixels(rotated,1,rotax);
     right=countpixels(rotated,rotax+1,size(rotated,2));
   else
      left=0;
      right=0;
   end
  l=evalvol(left);r=evalvol(right);
   volume=l+r;
else
   volume=0;
end
```

APPENDIX B

C Code

B.1. ssnap.c

```
#include <fcntl.h>
#include <stdlib.h>
#include <unistd.h>
#include <stdio.h>
#include <sys/mman.h>
#include <sys/ioctl.h>
#include <sys/time.h>
#include "ioctl_meteor.h"

#define ROWS 576
#define COLS 768
#define DEV "/dev/mmetfgrab0"
#define SRC METEOR_INPUT_DEV0
#define OFMT METEOR_GEO_RGB24
#define IFMT METEOR_FMT_PAL
#define CAP METEOR_CAP_SINGLE
#define FRAMES 1

int main(int argc, char **argv)
{
  FILE *fp = stdout;
  int noframes = 1;
  float pause = 5;
  int src = SRC, ifmt = IFMT, cap = CAP;
  int size = COLS * ROWS;
  struct meteor_frame_offset off;
  struct meteor_geomet geo;
  char *mem, *buf, str[11];
  int dev, i, j;
  unsigned char *ptr, *mmbuf;
  struct timeval time;
  struct timezone zone;
  double ot;

  if (--argc > 0)
   noframes = atoi(*++argv);
  if (--argc > 0)
   pause = atof(*++argv);

dev = open(DEV, O_RDONLY);
  geo.rows = ROWS;
  geo.columns = COLS;
  geo.frames = FRAMES;
  geo.oformat = OFMT;

ioctl(dev, METEORSETGEO, &geo);
ioctl(dev, METEORGFROFF, &off);
ioctl(dev, METEORSINPUT, &src);
ioctl(dev, METEORSFMT, &ifmt);

mem = mmap((caddr_t)0, off.fb_size, PROT_READ, MAP_PRIVATE, dev, (off_t)0);
gettimeofday(&time, &zone);
  ot = (double) (time.tv_sec + time.tv_usec/1e6 - pause);
fprintf(stderr, "Press Enter to start grabbing.");
getc(stdin);
gettimeofday(&time, &zone);
  for (j=0; j<noframes; j++)
   {
   while ((double) (time.tv_sec + time.tv_usec/1e6) < ot)
     gettimeofday(&time, &zone);
      ioctl(dev, METEORCAPTUR, &cap);
   fprintf(stdout, "Image:  %03d, sec:  %d, usec:  %d\n", j, time.tv_sec, time.tv_usec);
   mmbuf = (unsigned char *)(mem + off.frame_offset[0]);
ptr = buf = (unsigned char *)malloc(size * 3);
   for(i = 0; i < size;i++)
     {
       *(ptr + 2) = *mmbuf++;
       *(ptr + 1) = *mmbuf++;
        *ptr = *mmbuf++;
        ptr += 3;
        mmbuf++;
     }
   sprintf(str, "pic%03d.pnm", j);
   if (fp = fopen(str, "w"))
     {
       fprintf(fp,"P%c\n#Luleå University of Technology, The Visualization Project\n%d %d\n255\n",
'6', COLS, ROWS);
       fwrite (buf, 3 * sizeof(char), size, fp);
       fclose(fp);
       free(buf);
        ot = (double) (time.tv_sec + time.tv_usec/1e6 + pause);
     }
   }
munmap(mem, off.fb_size);
close(dev);
exit(0);
}
```